EFFECTS OF EXTREMELY LOW FREQUENCY ELECTROMAGNETIC FIELDS ON CASPASE ACTIVITIES

by

Mehmet Ozansoy

B.S., Molecular Biology and Genetics, Boğaziçi University, 1997

M.S., Molecular Biology and Genetics, Boğaziçi University, 2000

Submitted to the Institute for Graduate Studies in
Science and Engineering in partial fulfillment of
the requirements for the degree of
Doctor of Philosophy

Graduate Program in Molecular Biology and Genetics

Boğaziçi University

2006

ACKNOWLEDGEMENTS

I would like to express my sincere gratitude to my thesis supervisor Prof. Dr. A. Nazlı Başak for her guidance, unending encouragement and support throughout all my graduate years. I am also grateful to my thesis co-advisor Assoc. Prof. Yağmur Denizhan for her valuable criticisms and guidance in every step of this research.

I would also like to thank to Prof. Dr. Gülen Aktaş and Prof. Dr. Yani Skarlatos from Dept. of Physics for their help in constructing experimental systems that were used in this study.

I am very grateful to State Planning Organization for the financial support.

I would like to express my thanks to the members of my thesis committee, Prof. Dr. Mehmet Öztürk, Prof. Dr. Gülen Aktaş, and Assoc. Prof. Esra Battaloğlu for taking part in my thesis committee and for their valuable criticisms.

I would like to extend my thanks to the academic staff of the Dept. of Molecular Biology and Genetics for improving my knowledge

I am also very grateful to my mentors Ghazi Tadmouri and Onur Bilenoğlu.

I would like to thank all my friends in our lab. This study could not be completed without the pleasant friendship of Baki, Nagehan, Aslıhan, Caroline, Nazan, Ayşe, Mine, Sinem, Pınar and İzzet.

I would also like to thank my family for their patience, continuous support and encouragement they have provided throughout my life.

ABSTRACT

EFFECTS OF EXTREMELY LOW FREQUENCY ELECTROMAGNETIC FIELDS ON CASPASE ACTIVITIES

All life on Earth is bathed in a sea of natural low-frequency electromagnetic fields from conception to death. Since the World Health Organization (WHO) launched its international electromagnetic fields (EMF) project in 1996, it has conducted international reviews of the evidence on whether exposure to static and extremely low-frequency (ELF) fields might be harmful to health. ELF fields for WHO's EMF project are defined as those having frequencies above zero and below 300 Hz. In the framework of this study, the activation of seven different caspases will be investigated systematically, when extremely low frequency electromagnetic fields, which are thought to be an environmental hazard according to WHO, are applied to the HEK 293 cell line. The selected frequency will be 50 Hz, which is the power transmission line frequency in most parts of the world. Two different magnetic field strengths will be applied to HEK 293 cells, and two different exposure durations will be chosen. Caspase activity levels are to be measured at different time points after exposure. The common pattern seen in all of them was the oscillation of enzyme activities from the beginning. At 100 μT, caspases gave four peaks at four, eight, 16 and 34-hour incubation periods. This oscillatory behavior can also be seen when 25 μT magnetic field was applied, but the behaviors of the enzymes were different in a certain extent. The location and the number of the peaks at 25 μT exposure were quite variable, but the activity periods of all caspases seemed to be shorter than those exposed to 100 μT. The data presented here indicate that when ELF-EMF is applied to the HEK 293 cells, all seven caspases investigated are found to be activated, but this activation shows an oscillatory pattern, and in the long run it seems to be damped by some intracellular mechanisms.

ÖZET

AŞIRI DÜŞÜK FREKANSLI ELEKTROMANYETİK ALANLARIN KASPAZ AKTİVİTELERİNE ETKİSİ

Dünya üzerinde bulunan hayatın tamamı doğada bulunan düşük frekanslı elektromanyetik alanların etkisindedir. Dünya Sağlık Örgütü (WHO) 1996 yılında yapay olarak da üretilebilen bu tür elektromanyetik alanların sağlığa olan olası etkilerinin araştırılması için bir proje başlatmıştır. WHO aşırı düşük frekanslı elektromanyetik alanları, frekansları sıfırdan büyük, 300 Hz'den küçük alanlar olarak tanımlamaktadır. Bu çalışma çerçevesinde, HEK 293 hücrelerine 50 Hz frekansında, iki farklı manyetik alan şiddetinde elektromanyetik alanlar uygulanmış, ve uygulama iki farklı maruz kalma zamanı süresince yapılmıştır. Daha sonra elektromanyetik alanlara maruz bırakılan hücrelerde yedi farklı kaspaz enziminin aktiviteleri değişik zaman aralıkları ile ölçülmüştür. Enzim aktivitelerinde zamana bağlı bir dalgalanma bulunmuş, bu dalgalanmanın ana hatlarıyla hem 100 hem de 25 μT manyetik alan şiddetlerinde ortak olduğu saptanmıştır. Kaspazların hemen tamamı 100 μT'da dört farklı maksimum vermekte, ve bu tepe noktalarını yerleri zamansal olarak aynı gözükmektedir. 25 μT uygulandığında ise maksimumların yerleri ve büyüklükleri değişiklik göstermektedir. Sonuç olarak yapılan çalışma, aşırı düşük frekanslı elektromanyetik alanların HEK 293 hücrelerinde kaspaz enzimlerini aktive ettiğini göstermekte, ancak bu etkinin zamana bağlı bir şekilde dalgalandığı ve uzun dönemde sönümlendiği anlaşılmaktadır.

TABLE OF CONTENTS

LIST OF FIGURES

LIST OF TABLES

LIST OF SYMBOLS/ABBREVIATIONS

Ca^{+2}	Calcium ion
$\Delta\psi_m$	Mitochondrial membrane potential
Mg^{+2}	Magnesium ion
Mn^{+2}	Manganese ion
DNA	Deoxyribonucleic acid
HEK 293	Human embryonic kidney 293
Hz	Hertz
kDa	Kilo dalton
µl	Microliter
µT	Microtesla
ml	Milliliter
mM	Millimolar
mT	Millitesla
nm	Nanometer
nT	Nanotesla
PCD	Programmed cell death
rpm	Revolutions per minute
UV	Ultraviolet
V	Volt
V/m	Volt per meter

1. INTRODUCTION

1.1. Cell from a Systemic Perspective

Living systems are hierarchically organized, complex systems which are governed by nonlinear dynamics. Their behavior is nonlinear because the functioning of a living system cannot be explained as a mere superposition of the contribution of its subsystems. Very intuitively one can classify living systems as complex although the concept of complexity can be interpreted in many different ways. A possible definition of complexity has been provided by the biophysicist Robert Rosen in terms of the multitude of description. According to that definition a complex system requires a variety of irreducible descriptions, each of which corresponds to a distinct way of interacting with that system [1].

In multicellular organisms, the cell can be taken as the smallest unit of the organization in the sense that it exhibits metabolic activities that are essential for living. As a component of the hierarchically organized whole, a cell performs basic metabolic processes, like energy production, and protein turnover, and it responds to the signals received from the neighboring cells. Integrating external signals and signals emerging from the intracellular environment, it can reach a steady-state. This integration process requires a stringent control, and the easiest and most accessible device for it is the network of effectors (activators and inhibitors), acting upon a variety of regulated enzymes, proteins, receptors, and channels situated in strategic junctures of the overall system. Through the generalized intermolecular sharing of effectors, substrates and the products, functional blocks or modules are created, which can be easily adjusted to meet systemic demands. Furthermore, by performing interconnections between different signaling pathways, new instances of balance may be arranged at higher levels, regulating the drive towards cellular macro-states, like the onset of apoptosis, cell cycle progression and switching between different metabolisms.

1.1.1. The Modeling Relation and Complexity

Basically the modeling relation is the observer's "window" to the natural world. Figure 1.1 shows the modeling relation in a pictorial form. The figure reveals two systems, a so called "natural system" and a "formal system", related by a set of arrows depicting processes and/or mappings. The natural system is something which the observer would like to understand, as well as control and make predictions about. In particular, "arrow a" depicts causality in the natural world. Embedded in this representation is the notion that the world has some sort of order associated with it. The "arrow c" is called implication and represents some way in which the formal system is manipulated to try to mimic causal events in the natural system of interest. The "arrow b" is some way that the natural system is encoded, or some aspects of it are selected in terms of the formal system. Finally, the "arrow d" is a way to decode the result of the implication event in the formal system to see if it represents the causal event's result in the natural system. When the integration of the relations "b", "c", and "d" gives the relation "a", then it can be said that the diagram commutes and that the model of the natural system is produced [1].

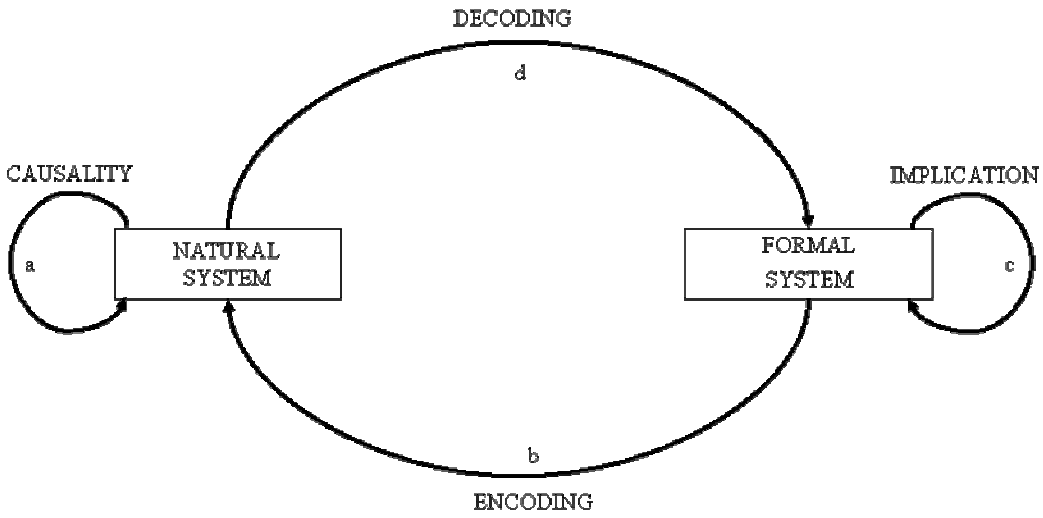

Figure 1.1. The modeling relation [1].

The programmed cell death and/or apoptosis is a network of processes regulated intracellulary and extracellularly, and using the above mentioned modeling relation, it corresponds to the natural system, and the experimental setup constructed corresponds

to the formal system. Measurements made on the formal system can be used to explain the behaviors seen in the natural system with an approximation only, because of the limitations imposed by the modeling relation itself, and the limitations of the experimental setup, which are unavoidable when compared with the natural system.

1.2. Programmed Cell Death

Programmed cell death (PCD) is one of the central themes in development, participating in particular in morphogenesis, in sexual differentiation, and in the epigenetic self-organization processes that allow the emergence of the two most complex regulatory organs, the immune system and the nervous system. PCD is also crucial in the adult, by allowing tissue homeostasis, elimination of damaged or abnormal cells, and defense against infections. On the other hand, PCD dysregulation has been proposed to participate in the pathogenesis of several diseases, ranging from cancer and autoimmunity to infectious diseases and neurodegeneration.

Cell death processes have been successively named “chromatolysis”, “pyknosis”, “karyolysis”, “karyorhexis”, “shrinkage necrosis”, “programmed cell death”, “cell suicide”, “self destruction” and “apoptosis”. The terms “programmed cell death”, “cell suicide” and “apoptosis” have each played a major role in expressing crucial conceptual advances concerning cell death, but it should also be noted that none of these terms are synonymous and each one carries its own metaphors and implications, and hence some degree of ambiguity.

Etymologically, the term “program” means “pre-written”. Therefore, the very concept of the program, in biology, is ambiguous, suggesting a framework of design and finality, within which the existence of pre-written genetic information can easily be confused with multiple ways it can be used by the cells and the body. It is not the individual fate of each cell, its survival or its death, that is programmed, but the capacity of each cell to induce or repress its self-destruction, depending on its present and past interactions with the other cells that constitute the body, and on the integrity of its internal components. The concept of “cell suicide” or “self-destruction” also provides some level of ambiguity, not only because its obvious anthropomorphic

reference, but also because it favors a confusion between the act of initiating self-dismantling, which the cell indeed performs by activating an intrinsic cell death machinery, and both the "decision" to kill itself and the implementation of the death process, which depends on the nature of interactions between the cell and the body, rather than on the cell itself. Finally, the term "apoptosis" (etymologically, the "fall", as that of leaves in autumn), while implicitly perceived as describing the death process itself, describes actually a phenotype; the stereotyped series of modifications usually associated with programmed cell death. These various changes involve cell shrinkage, plasma membrane blebbing with partial maintenance of impermeability, permeabilization of mitochondrial outer membrane, nuclear chromatin condensation and fragmentation, genomic DNA fragmentation, cytoskeletal modifications, and segmentation of the cell into apoptotic bodies. Although apoptosis is the most typical and frequent phenotype of self-destruction, it is not the only one. For this reason, the term "apoptosis" should not be considered as a synonym of the terms "programmed cell death", "cell suicide" or "self-destruction". The common usage of these terms as identical can cause a failure to differentiate between the nature of the effectors that may be responsible for the execution of cell death, and the effectors that are responsible for the execution of apoptotic phenotype, while not being obligatorily the cause of death [2].

1.2.1. Programmed Cell Death from Evolutionary Perspective: Sine Qua Non of a Multicellular State

The origin of eukaryotes and the advent of multicellularity are evolutionary transitions that involved invention of several fundamentally new functional systems. Programmed cell death apparatus is such a major eukaryotic innovation, which does not appear to have direct prokaryotic predecessors. Although bacterial cells commit suicide under certain circumstances, for example, during fruiting body formation in Myxobacteria, these mechanisms do not appear to be essential for the survival of prokaryotes in general, and their molecular build-up seems to be unrelated to that of eukaryotic apoptotic machinery. In contrast, in multicellular eukaryotes, programmed cell death appears to be universally present and indeed it should be regarded as one of the hallmarks of the multicellular state itself.

Three, not mutually exclusive, paths can be envisaged for the origin of eukaryotic functional systems, for example programmed cell death, that do not have counterparts in prokaryotes. First, an existence of cryptic prokaryotic precursor, i.e. an ancestral system in prokaryotes with the same or similar function as the novel eukaryotic system. Secondly, recruitment of prokaryotic proteins (domains) whose original functions in prokaryotes are unrelated to the new functions in eukaryotes, but whose biochemical activities could be employed towards those functions, would happen. Finally, there can be evolution of new, eukaryote-specific proteins (domains) for the new functions.

The phylogenetic analyses for the key components of the eukaryotic PCD system revealed that the enzymes involved in apoptosis tend to show a broad phyletic distribution, with bacterial homologs identifiable, whereas the non-enzymatic components are less conserved, and they are often limited in their distribution to only one eukaryotic lineage. The feature of these phylogenetic patterns that appears to be critical for the understanding of the origin and evolution of eukaryotic PCD is that the prokaryotic homologs of the proteins involved in PCD are widely represented in bacteria, but not in archaea. This pattern suggests the possibility of a substantial contribution of acquired bacterial genes to the evolution of the eukaryotic PCD system [3].

1.2.2. The Nature of Apoptosis and Its Regulation

Apoptosis can be initiated by various external or internal signals and executed through several interrelated signaling pathways. At the molecular level, the apoptotic machinery forms a complex cascade of ordered events, controlled by the regulated expression of apoptosis-associated genes and proteins. It is the concerted action of these components that finally results in cell dismantling and in the formation of apoptotic bodies.

The key to understand apoptosis is the activation and function of a set of proteases, the cysteine dependent aspartic acid proteases (caspases) (Table 1.1). When the caspases are activated, they cleave a wide variety of proteins, including certain key

substrates in the cell. Caspases are synthesized as a single-chain of inactive zymogens, consisting of four domains; an amino-terminal prodomain of variable length, a large

Table 1.1. Mammalian caspases and their general characteristics [4].

Name of the Enzyme	Size of Enzyme Precursor (kDa)	Prodomain Type	Active Subunits (kDa)
Apoptotic Initiator Caspases			
Caspase-2	51	Long, with CARD region	19/12
Caspase-8	55	Long, with two DED regions	18/11
Caspase-9	45	Long, with CARD region	17/10
Caspase-10	55	Long, with two DED regions	17/12
Caspase-12	50	Long, with CARD region	20/10
Apoptotic Executioner Caspases			
Caspase-3	32	Short	17/12
Caspase-6	34	Short	18/11
Caspase-7	35	Short	20/12
Inflammatory Caspases			
Caspase-1	45	Long, with CARD region	20/10
Caspase-4	43	Long, with CARD region	20/10
Caspase-5	48	Long, with CARD region	20/10
Caspase-11	42	Long, with CARD region	20/10
Other Mammalian Caspases			
Caspase-14	30	Short	20/10

subunit with molecular weight of about 20 kilodalton (kDa), a small subunit (~10kDa), and a linker region connecting these catalytic subunits. The linker region is missing in some family members. Proteolytic cleavage of the caspase precursors results in the separation of large and small subunits with the production of a heterotetrameric complex (the active enzyme) consisting of two large and two small subunits. Caspases differ in the length and in the amino acid sequence of their amino-terminal prodomain, which is either short (20-30 amino acid residues) or long. The long prodomain (more than 90 amino acid residues) contains one of two modular regions essential for the interaction with adaptor proteins. These modules contain death effector domains (DED) and caspase recruitment domains (CARD) [5, 6, 7, 8].

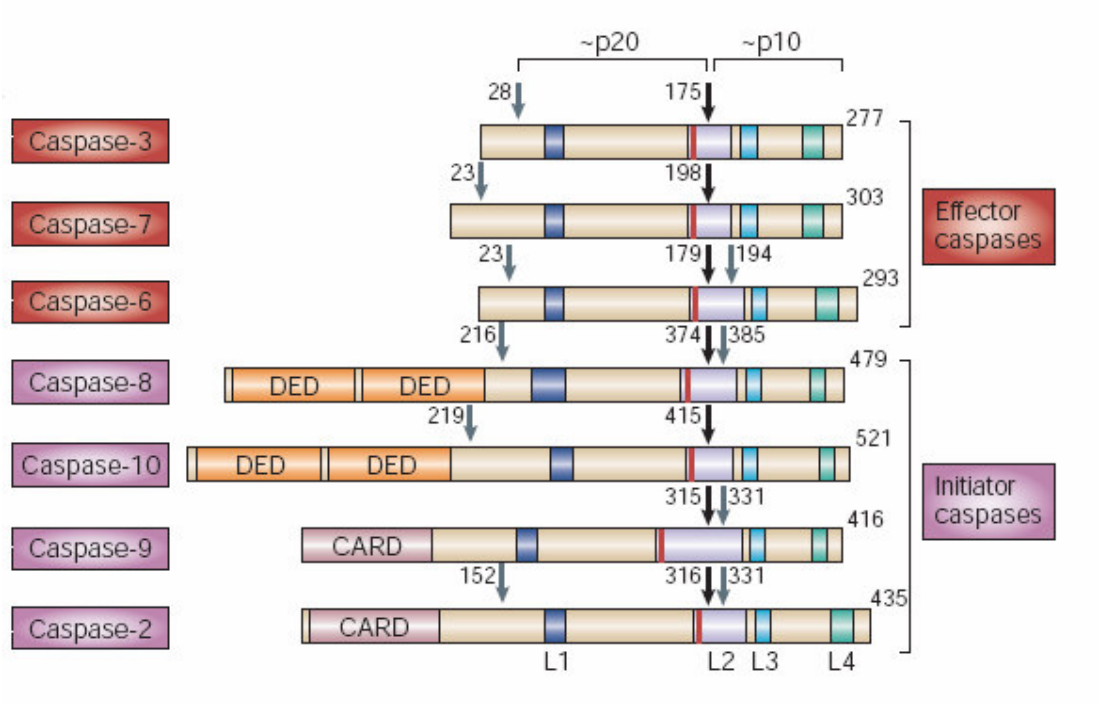

Figure 1.2. Apoptotic caspases. The positions of the first intra-chain activation cleavage and other sites of cleavage are represented black and grey arrows respectively. The four surface loops (L1-L4) that shape the catalytic groove indicated. The catalytic residue Cys is shown as a red line at the beginning of L2 [9].

Based on their proapoptotic functions, the caspases have been divided into two groups: Initiators and executioners. Initiator caspases (caspases-2, -8, -9, -10, and, probably, -11) activate the second group of caspases (caspases-3, -6, and -7) (Figure

1.2). The executioner caspases are able to directly degrade multiple substrates including the structural and regulatory proteins in the cell nucleus, cytoplasm, and cytoskeleton. Caspases-1 and -4, -5 have similar structures, and they are predominantly involved in the maturation of proinflammatory cytokines. The caspase proteolytic signaling cascades are interconnected and due to overlapping substrate specificity they are also partially redundant. As a result, the apoptotic signal can be significantly amplified. The caspase activation cascade is achieved by using two basic pathways; the mitochondrial pathway and the death receptor pathway [10, 11, 12].

1.2.3. The Role of Mitochondria in Apoptosis

It has been apparent that apoptosis and other forms of cell death are often controlled at one or more crucial steps involving the mitochondria. The basic mitochondrial pathway of apoptosis in vertebrates begins with the permeabilization of the mitochondrial outer membrane by proapoptotic members of the B-cell lymphoma gene 2 (Bcl-2) family, initially by a subset of these called the "BH3-only subfamily" proteins because they possess only one of the Bcl-2 homology (BH) domains. These include Bid, Bim, Harikari, Noxa, and a number of others. In response to environmental cues these proteins interact with another set of proapoptotic Bcl-2 members, the Bax subfamily, including Bax, Bak, and probably Bok, loosely residing on the mitochondrial outer membrane or in the cytosol [5, 6, 13]. The interaction causes the Bax subfamily proteins to oligomerize and to insert into the mitochondrial membrane. The resulting complex (permeability transition pore complex, PTPC) acts to trigger the sudden and complete release of proteins, including cytochrome c, from the intermembrane space into the cytosol. The PTPC functions as a sensor for eight different parameters. First is the voltage; the PTPC decodes voltage changes into variations of the probability (the gating potential) at which pore opening occurs. Pore agonists shift the gating potential to more negative values (physiological value 200 mV, negative inside), favoring pore opening, whereas pore antagonists favour its closure. Second parameter is divalent cations; mitochondrial matrix Ca^{+2} increases the probability of pore opening, matrix Mg^{+2} or Mn^{+2} and external divalent metal ions including Ca^{+2} all decrease the probability of pore opening. The third parameter is the matrix pH; the permeability pore is closed at neutral or acidic pH owing to reversible

protonation of histidine residues and/or inhibition of the interaction between matrix cyclophilin and the adenine nucleotide translocator (ANT). Alkalinization is permissive for pore opening with a maximum effect at a matrix pH of approximately seven. The fourth parameter is the thiol oxidation; oxidation (disulphide formation) of a critical mitochondrial dithiol increases the probability of pore opening. The redox status of this dithiol is in equilibrium with that of matrix glutathione. Another parameter is the oxidation/reduction state of pyridine nucleotides ($NADH/NAD^+$ and $NADPH/NADP^+$). Oxidation of pyridine nucleotides favours permeability transition. The endogenous ANT ligand adenosine diphosphate (ADP) as well as bongkrekate inhibit permeability transition. Atractyloside, another ANT ligand, induces permeability transition. The fifth parameter is the metabolites; glucose and creatine inhibit permeability transition, presumably through their action on hexokinase and creatine kinase. Coenzyme Q also inhibits permeability transition. Long chain fatty acids, ceramide and ganglioside GD3 favour permeability transition. The last parameter is anti- and proapoptotic members of the Bcl-2 family [13].

The PTPC is formed at the contact site between the inner mitochondrial membrane and the outer mitochondrial membrane. Its core components are the ANT, found in the inner mitochondrial membrane, and the voltage-dependent anion channel (VDAC), located in the outer mitochondrial membrane. The VDAC is normally permeable to solutes of up to five kDa, allowing the free exchange of respiratory chain substrates between the mitochondrial intermembrane space and the cytosol. In contrast, the inner mitochondrial membrane is almost impermeable, a feature that is essential for generation of the electrochemical proton gradient ($\Delta\psi_m$) used for oxidative phosphorylation. Many studies reveal that apoptosis correlates with signs of a permeability transition, such as loss of the mitochodrial transmembrane potential ($\Delta\psi_m$) [13].

The process of mitochondrial outer membrane permeabilization depends entirely on the function of Bax and Bak to disrupt the barrier function of the outer membrane. Bax in its native, cytosolic, and monomeric form is not constitutively active but it must be activated if it is to permeabilize the mitochondrial outer membrane. The activation of Bax can be triggered by BH3-only proteins, but there appears to be specificity in this

interaction. Only Bid and Bim have this function, whereas others (Bad, Puma, Noxa, Hrk) appear to perform their function through neutralization of antiapoptotic Bcl-2 proteins. One model for permeabilization of mitochondrial outer membrane holds that oligomerized Bax and Bak may form pores capable of releasing cytochrome c. This thesis has origins in the structural similarity between Bcl-2 family molecules and the pore-forming helices of bacterial toxins [13, 14, 15].

The released cytochrome c binds to apoptotic protease activating factor 1 (Apaf-1), a monomeric cytosolic protein. This induces a conformational change of Apaf-1 leading to its oligomerization, and recruitment of procaspase-9 to form apoptosome, and in the presence of dATP/ATP, it activates procaspase-9. The active caspase-9 recruits and activates the executioner procaspase-3. The cytoplasmic efflux of cytochrome c is the key event in the activation of the mitochondria-dependent (intrinsic) death pathway. The ratio between antiapoptotic (Bcl-2, Bcl-$_{XL}$, Bcl-w, etc.) and proapoptotic (Bax, Bak, Noxa, etc.) Bcl-2 family members determines life or death decisions of the cell in this pathway. Their expression level and activation stage can strongly influence the release of apoptogenic molecules like cytochrome c, procaspase-2, -3, -9, the apoptosis inducing factor (AIF), endonuclease G, the second mitochondria derived activator of caspase/direct IAP binding protein with low pI (Smac/DIABLO), the high temperature requirement A2 (Omi/HtrA2), and many others from the mitochondrial intermembrane space [5, 6, 7, 13, 14, 15].

Both caspase activation and activity in the cell are tightly controlled. Naturally occurring direct caspase inhibitors include seven members of the mammalian inhibitors of apoptosis (IAPs) family of proteins, FADD-like ICE-inhibitory protein (c-FLIP), bifunctional apoptosis regulator (BAR) and apoptosis repressor with CARD (ARC) (Table 1.2). It should be noted that expression of caspase inhibitors except for XIAP, and to a lesser extent c-IAP1 and c-IAP2, are tissue specific. All the IAP family proteins share a specific baculoviral IAP repeat region (BIR) of about 70 amino acid residues required to provide the antiapoptotic effect. All IAPs, except for ILP-2, can preferentially bind to active forms of caspase-3, and caspase-7 but not to their precursors. XIAP, ILP-2 and livin can also inhibit caspase-9. c-FLIP, BAR, and ARC prevent transduction of the proapoptotic signal from death receptors targeting another

apical caspase, caspase-8. Intriguingly, BAR is able to inhibit cell death in response to a broad range of cell death stimuli inducing apoptotic pathways via mitochondria, death receptors, or as a result of endoplasmic reticulum stress (ER). Therefore, individual caspase inhibitors contribute to cell death machinery in cell type- and cascade-specific manner [5, 6, 7, 16, 17, 18, 19].

Table 1.2. Basic properties of some endogenous caspase inhibitors [4].

Name of the Protein	Molecular Weight (kDa)	Domain Structures	Caspase Specificity
NAIP (BIRC1)	156	BIR1, BIR2, BIR3, NOD	Caspase-3 and -7
c-IAP1 (BIRC2)	70	BIR1, BIR2, BIR3, CARD, RING	Caspase-3 and -7
c-IAP2 (BIRC3)	68	BIR1, BIR2, BIR3, CARD, RING	Caspase-3 and -7
XIAP (BIRC4)	57	BIR1, BIR2, BIR3, RING	Caspase-3, -7 and -9
Survivin (BIRC5)	17	BIR	Caspase-3 and -7
Livin (BIRC7)	31	BIR, RING	Caspase-3, -7 and -9
ILP-2 (BIRC8)	25	BIR, RING	Caspase-9
c-FLIPL (I-FLICE)	55	DED, DED, pseudo-caspase domain	Caspase-8 and -10
ARC	30	CARD	Caspase-2 and -8
BAR	46	RING, SAM, DED	Caspase-8

The antideath function of the IAP family proteins can be blocked by specific inhibitors. After the initiation of apoptosis, Smac/DIABLO and Omi/HtrA2 proteins are released from mitochondrial intermembrane space. Both Smac and Omi contain IAP binding motifs (IBMs) through which they bind to IAPs and release IAPs bound caspases. The overexpression of Smac or Omi in the cells increases their sensitivity to induction of apoptosis by UV radiation [5, 6, 7].

1.2.4. Receptor-Mediated Apoptosis

Death receptors located on the cell membrane, rely on signaling proteins possessing a distinct set of modular protein motifs capable of homotypic interaction, including death domains (DD) and death effector domains (DED). Structural studies of DD and DED domains have revealed that their overall folding pattern is very similar to that of the CARD domain, indicative of an evolutionarily conserved structure in the assemblage of proapoptotic cascades.

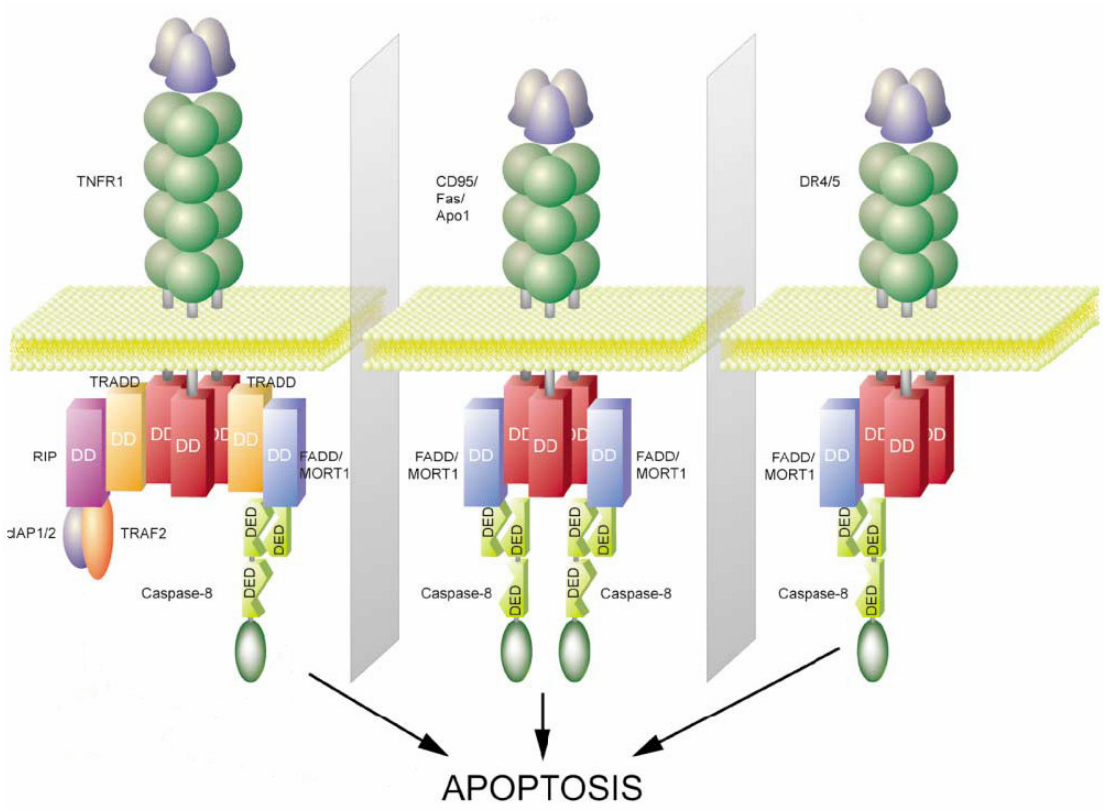

Figure 1.3. Extrinsic death receptor pathways. The distinct composition of the DISC downstream of the vatious death receptors TNFR1, CD95 and DR4/5 is illustrated [7].

Death receptors, such as Fas/CD95 as well as tumor necrosis factor receptor-1 (TNFR1) trigger caspase activation through a different type of apoptosome, one that is assembled and resides on the cytosolic region of the death receptor itself (Figure 1.3). Upon ligation, the death receptor undergoes a conformational change, a signaling complex known as death-inducing signaling complex (DISC) is formed. The adaptor

protein FADD/MORT, bearing both DD and DED motifs, binds to the DD of the receptor and recruits procaspase-8 or procaspase-10 via its DED domain. Activation of caspase-8 in the DISC complex is believed to follow an "induced proximity" model, where high local concentration of procaspase-8 leads to its autoproteolytic activation and subsequent activation of caspase-3 and caspase-7. Caspase-8 can also activate a proapoptotic protein, Bid, through cleavage, and truncated Bid (tBid) facilitates the formation of the PTPC in mitochondria (Figure 1.4) [7].

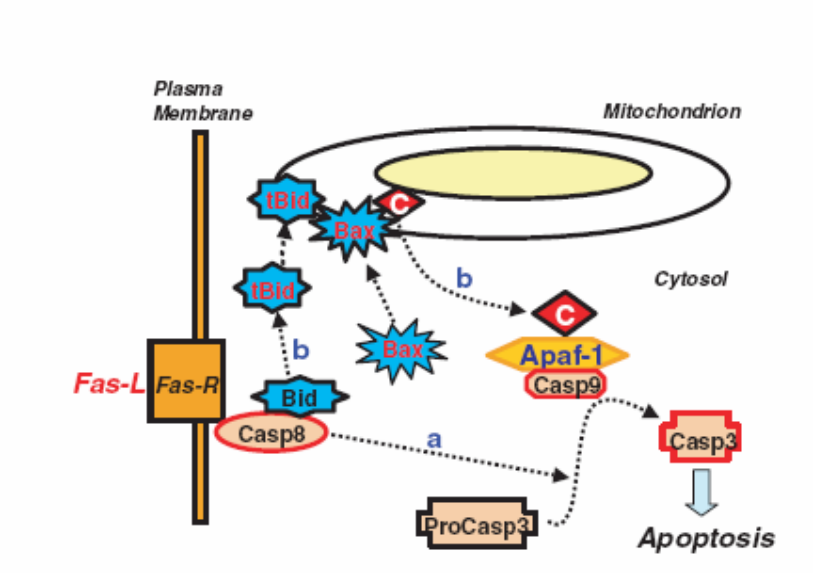

Figure 1.4. Convergence of receptor mediated apoptosis signaling with mitochondrial pathway.

Another set of death receptors (DR 4/5) have been characterized that share a different death ligand, known as Apo2L, TNF-related apoptosis inducing ligand (TRAIL). DISC complex formation and Bid cleavage downstream of DR 4/5 are similar to the Fas pathway.

1.2.5. Late Stages of Apoptotic Process

Condensation and fragmentation of nuclei is a morphological hallmark of apoptosis. Downstream of caspase activation, degradation of DNA first occurs at A/T rich regions within the nuclear scaffold sites to produce 50-200 kb fragments. A caspase-activated DNase (CAD) degrades the genomic DNA, after it is cleaved by

caspases-3 and -7. In mammalian cells, caspase-independent apoptotic DNA degradation has been attributed to two mitochondrial proteins, endonuclease G and AIF, that translocate to the nucleus upon release. AIF induces nuclear condensation and large scale DNA fragmentation. Genetic studies indicate that nuclear translocation of AIF is dependent on poly-ADP ribose polymerase-1 (PARP-1). PARP-1 attaches poly ADP-ribose to nuclear proteins such as histones, and its activation leads to apoptosis under several conditions, including DNA damage. AIF function, in turn, is required for PARP-1 proapoptotic activity [5.6].

The apoptotic pathway and the engulfment of the dying cell are part of a continuum, that helps ensure the noninflammatory nature of this death paradigm. Phagocytes recognize the surface of the dying cell most likely through a signal such as phosphatidylserine displayed on the plasma membrane. Evidence shows the participation of multiple engulfment receptors including CD-91, CD-14, CD-36, and $\alpha_V\beta_3$ integrin, as well as the phosphatidylserine receptor. In addition to engulfment of apoptotic cells, macrophages are important regulators of proinflammatory responses by releasing cytokines such as tumor necrosis factor α (TNFα). While proinflammatory factors are necessary in immune reaction against infection, their suppression during apoptotic corpse clearence is essential [7].

1.3. Biological Effects of Electromagnetic Fields

Electromagnetic fields are generated by accelerating electric charges. The radiated fields consist of oscillating electric and magnetic fields, which are at right angles to each other and also to the direction of field propagation. Thus, electromagnetic fields are transverse in nature. Maxwell's theory about electromagnetic fields shows that the electric and magnetic field amplitudes in an electromagnetic field are related, and at large distances from the source, the amplitudes of the oscillating fields diminish with distance. The radiated waves can be detected at great distances from the oscillating charges. Furthermore, electromagnetic fields carry energy and momentum and hence exert pressure on a surface.

Electromagnetic fields cover a wide range of frequencies (Figure 1.5). For example, radio waves (frequencies of about 10^7 Hz) are electromagnetic waves produced by oscillating currents in a radio tower's transmitting antenna. Light waves are a high frequency form of electromagnetic radiation (about 10^{14} Hz) produced by oscillating electrons within atomic systems.

All life on Earth is bathed in a sea of natural low-frequency electromagnetic fields from conception to death. Generated principally by thunderstorm activity in equatorial zones, these fields exhibit peaks in the extremely low-frequency (ELF)

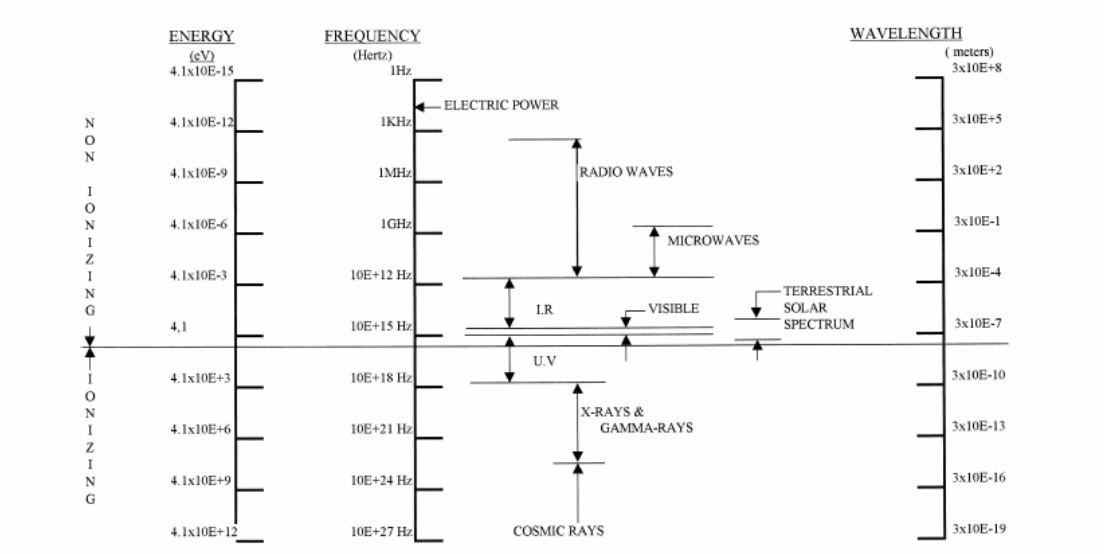

Figure 1.5. Spectrum of electromagnetic waves. UV: Ultraviolet, IR: Infrared [20].

spectrum between eight and 32 Hz, called the Schumann resonances. Their energy is measured in billions of coulombs, and they are ducted worldwide between the Earth's surface and the ionosphere approximately 140 km above the Earth. With a circumference of 41,000 km, the Earth may act as a cavity resonator in this ducted propagation, with a resonant frequency around eight Hz for waves moving at the velocity of light. Schumann fields are weak, with electric components of about 0.01 V/m, and magnetic fields of one-10 nT. These fields are very weak when compared with the Earth's static geomagnetic field, typically around 50 μT [21].

1.3.1. Health Risk Assessment of ELF Fields

Since the World Health Organization (WHO) launched its international electromagnetic fields (EMF) project in 1996, it has conducted international reviews of the evidence on whether exposure to static and extremely low-frequency fields might be harmful to health. ELF fields for WHO's EMF project are defined as those having frequencies above zero and below 300 Hz [22].

When electric power is used, the conductors carrying the current are surrounded by magnetic fields (MFs). The frequency of the field is determined by the frequency of the alternating current, which is 60 Hz in North America and 50 Hz elsewhere. The waveform of the MFs produced by alternating current is sinusoidal. The intensity of a magnetic field is usually expressed as magnetic flux density in microtesla or millitesla. For MFs with sinusoidal waveforms, the flux density is normally expressed as the root-mean-square (rms) value, but many studies describe the intensity of non-sinusoidal waveforms by giving the amplitude from the bottom to the top of the wave, the so-called peak-to-peak (p-p) value [20].

To date, the only mechanism of action of ELF fields in biological tissues that appears to have health consequences is the induction of electric currents and fields. The magnitude of induced currents and fields in the body is a limiting factor for setting human exposure guidelines to static and ELF fields in current international standards. WHO categorizes ELF fields as category 2B, according to the classification of International Agency for Research on Cancer (IARC), meaning that ELF fields are possibly carcinogenic to humans. Other examples of agents contained in this category are coffee, pickled vegetables, gasoline engine exhaust, glass wool and styrene [22].

ELF fields are also categorized as non-ionizing radiation, because of the low energy they carry, and it has been considered that they could not have adverse effects on living organisms because they could not exert any thermal effect on them. However, many studies have revealed that these non-ionizing fields would have some effects on

several cellular systems, like signal transduction, protein synthesis/gene expression, and enzyme action, and these effects are called athermal.

1.3.2. Teratogenic and Reproductive Effects of ELF Fields

Both epidemiological and animal studies indicate that low-frequency magnetic fields do not have strong effects on embryonal development. No gross malformations have been found in animal studies, and epidemiological studies have not shown evidence of an excess of birth defects. There is some epidemiological evidence of an increased risk of spontaneous abortion, and experimental studies have also provided suggestive evidence of increased fetal loss (resorptions) in a strain-specific manner.

It has been suggested that deficits in body weight are sensitive indicators of developmental toxicity. Some animal studies have indicated decreased fetal weight or size, but most studies have shown no changes. The epidemiological data available on low birth weight or intrauterine growth retardation are very limited, but no statistically significant effects have been reported.

Slight increases have been reported in any parameters used for measuring embryonal damage, suggesting that maternal MF exposure might affect only a small portion of embryos. This may indicate that MFs are embryotoxic only together with other environmental or genetic risk factors. The epidemiological studies on the effects of paternal exposure are contradictory and inconclusive. The results of the multigeneration animal studies do not suggest any major effects of MF on male reproduction.

In epidemiological studies, some effects have been reported at ELF magnetic flux densities below one microtesla. However, the field intensities should not be directly compared without considering the interaction mechanisms. Direct comparison of the intensities at the same frequency is possible only if it is assumed that the biological effects of MFs are based on direct magnetic interaction. If the bioeffects are caused by the electric currents induced by MF, then body size and orientation should also be taken into account.

The biophysical and biological mechanisms by which low-frequency MFs could affect reproduction and development are not known. Several hypothetical mechanisms have been proposed, and ELF magnetic fields have been reported to affect many cellular processes, including, signal transduction, cell proliferation and intercellular communication. Such effects could theoretically disturb embryonal development and/or implantation processes [23].

1.3.3. Carcinogenic Effects of ELF Fields

In the multistage model of carcinogenesis, the three operationally defined stages in tumor formation are initiation, promotion and progression. Initiation is the interaction of a genotoxic carcinogen (initiator) with the DNA of a cell, resulting in cytogenetic damage that leads to mutation. In addition to initiation by chemical agents or ionizing radiation, the process of initiation is thought to encompass the actions of inherited mutations, cancer-causing viral genes and altered cellular genes (oncogenes). The damaged DNA may revert to normal if DNA repair mechanisms operate successfully; if not, the transformed (initiated) cells may grow into a tumor that becomes clinically apparent. This is dependent on the presence of promoting stimuli. In other words, the initiated cells may remain dormant or latent awaiting a promoting stimulus before a tumor results. Promotion by systemic factors (hormones and other growth enhancing factors) or exogenous factors (environmental) involves facilitation of the growth and development of dormant or latent tumor cells. Thus, a promoter or co-carcinogen is usually not a carcinogen by itself, but it potentiates the effects of a carcinogen. In addition of promoting factors, co-promoting factors may play a role in carcinogenesis. Co-promoting factors are not tumor promoters, but enhance tumor promotion in response to promoters [24].

Numerous in vitro studies have indicated that 50 and 60 Hz MFs are not mutagenic, namely, they are not initiators in carcinogenesis, but may act to facilitate promotion and progression of tumors, and possibly interfere with DNA repair, thereby inducing co-carcinogenic effects. In vitro findings from MF exposure of cell cultures which may be relevant in this respect, involve alterations in gene transcription and

protein synthesis, increases in ornithine decarboxylase (ODC) activity, stimulated cell growth and proliferation, alterations in intercellular communication, and effects on Ca^{+2} homeostasis which may have implications for oncogene activation and immune responses [25, 26, 27].

Recent investigations have revealed that MF alters β-adrenergic receptor activity via interfering cyclic adenosine monophosphate (cAMP) accumulation of primary osteoblast-enriched bone cells from five day old mice, when they are treated with 100 μT, 60 Hz sinusoidal MF. In addition to that, MF exposure changes protein kinase C (PKC) activity; PKC is a key enzyme in the signal transduction cascade, and with regard to cancer, PKC represents the cellular receptor for phorbol esters which are a potent class of tumor promoters. Exposure of 50 Hz, pulsed (eight mT peak) MF resulted in significant activation of PKC compared to control cells [28].

Evidence for 60 Hz MFs increasing Ca^{+2} during signal transduction in lymphocytes has been reported. A 60-minutes exposure of rat thymic lymphocytes to a 22 mT MF has been performed in the presence or absence of concanavalin-A, a mitogen which is believed to interact with the T-cell receptor. Non-activated cells (no mitogen) were unresponsive to the MF; Ca^{+2} influx has not been altered. When concanavalin-A was present, the MF led to a significant increase in Ca^{+2} influx. It appears that the level of mitogen activation is critical for the MF effect on calcium influx [29, 30].

Another important finding is that c-myc mRNA transcripts were found to be elevated by MFs in a HL-60 cell line treated with 60 Hz sinusoidal MF. The oncogene myc belongs to a set of cellular messengers commonly referred to as “immediate early response” genes, since their expression is activated by a variety of mitogenic stimuli, independent of de novo protein synthesis. The protein products of immediate early response genes such as myc are thought to facilitate progression of the cell through the cell cycle and synthesize DNA in S phase [31].

A recent study about ODC activity has revealed a change in the activity of the enzyme when MFs were applied. ODC is the controlling enzyme in the polyamine

synthesis pathway, and it is regulated by a wide variety of growth factors and mitogens at the cell surface; it is unique in its ability to change rapidly in response to extracellular signals. ODC activity is increased by exposure to a 60 Hz MF in mouse L929 cells with MF intesities of 10 μT, and a maximal enhancement has been produced by four hours exposure [32]. Another finding about ODC activity is that three different cell lines (human promyelocytic leukemia HL-60, mouse ascites tumor ELD, and mouse teratocarcinoma F9) show elevated levels of ODC in response to 30 μT, 50 Hz MF. The magnitude of ODC elevation varied across cell lines (20 per cent for HL-60 cells, to 5-6 fold for ELD cells), and factors such as serum and protein (bovine serum albumin) appeared to play a role in ODC activity in the MF [33].

Liburdy and colleagues reported that human breast cancer cell growth can be altered by a 1.2 μT, 60 Hz MF in vitro. In these studies the hormone, melatonin, has been employed to inhibit breast cancer cell growth and cells have been exposed to MF. In the absence of melatonin, MCF-7 cells grew identically in 0.2 or 1.2 μT MF. The experiments were repeated with cells in the presence of physiological concentrations of melatonin and in the presence of 0.2 μT MFs. MCF-7 cells showed a significant inhibition of growth during a seven-day growth cycle. When a 1.2 μT MF was employed with melatonin, the natural oncostatic action of melatonin was completely blocked. Thus, in the presence of MF, melatonin was ineffective in inhibiting growth of MCF-7 cells. Conversely, when melatonin was absent in the cell culture media, the 1.2 μT MF did not affect MCF-7 cell proliferation. These findings indicate that a 1.2 μT MF can act to enhance breast cancer cell proliferation by blocking melatonin's action on cell growth. At present, it is not known precisely, what target molecule(s) the MF interacts with, to trigger a blocking of melatonin's action [34].

1.3.4. Interaction of DNA with ELF Fields

Low frequency electric fields do not penetrate cells very effectively because of the low dielectric constant of the cell membrane, but low frequency magnetic fields do penetrate cells. The electric fields they induce in cells are very small because of cell dimensions, so an indirect route via the membrane has been assumed.

Direct interaction of magnetic fields with DNA and the more generally accepted signal transduction cascade initiated at the cell membrane can both lead to signal amplification. In the membrane hypothesis, signal transduction is via cascades utilizing protein kinases. In the direct interaction with DNA, signal transduction is by interaction with large electron flows. Several mechanisms have been proposed for the initial interaction of magnetic fields with cells, but the most likely explanation is the mobile charge interaction (MCI) model, which proposes that the interaction of a magnetic field with a moving charge leads to a change in its velocity. Interaction of magnetic fields with moving charges has been shown in enzymes. In line with field induced changes observed in enzyme activities, it is suggested that MFs interact with moving electrons in the stacked bases of DNA. Magnetic field-induced increases in transcript levels have been demonstrated despite the low calculated forces that are predicted to be insufficient to affect a DNA chain. The forces induced by magnetic fields may be large enough to affect processes that can change the rate of movement of electrons significantly, and thereby initiate changes in the DNA [35, 36].

It has been shown experimentally that acute exposure of rats to a 60 Hz MF with flux densities 0.1, 0.25, and 0.5 mT cause a dose dependent increase in DNA strand breaks in brain cells of animals. An increase in single-strand breaks has been observed after exposure to MFs of 0.1, 0.25,and 0.5 mT, whereas an increase in double-strand breaks have been observed at 0.25, and 0.5 mT [37, 38, 39, 40, 41, 42, 43].

1.3.5. Effect of ELF Fields on Apoptosis

Evidence of the possible effects of ELF fields on apoptosis is very limited. One study applying MF of 50 Hz with different field intensities on transformed (human squamous cell carcinoma, SCLII) and nontransformed (human amniotic fluid cell line, AFC) cell lines revealed that a statistically significant increase in micronucleus formation frequency, being an indicator of apoptosis, and in apoptosis in SCLII cells after 48 and 72 hours continuous exposure to 0.8 and 1.0 mT has been found. However, exposure to AFC cells to MFs of different intensities at 50 Hz showed no statistically significant differences compared with controls [44]. Another study with rat tendon fibroblast (RTF) and rat bone marrow (RBM) osteoprogenitor cells showed that 60 Hz,

0.25 mT MF results in extensive detachment of preattached cells and prevented the normal attachment of cells not previously attached to substrates [45]. In addition, the same MF causes the formation of apoptotic morphologies on both cell types. A study using two transformed cell lines (WiDr, human colon adenocarcinoma, and MCF-7, human breast adenocarcinoma) and one nontransformed cell line (MRC-5, embryonal lung fibroblast) exhibited that 50 Hz MF with more than 1.0 mT induces cell death induction morphologically consistent with apoptosis on the two transformed cell lines [46]. On the other hand, there was no statistically significant difference between the nontransformed cell line exposed to the same MF and the control cells. In contrast to these evidence favoring the positive relation between the ELF fields and apoptosis, a study using human neuroblastoma cell line (LAN-5) revealed that MF with 50 Hz, 1.0 mT did not have any effect on apoptosis induction. Furthermore, this exposure showed a slight and transient increase of B-myb oncogene expression and a small increase in proliferation index [47].

2. PURPOSE

Caspases, the cysteine-dependent aspartic acid proteases, are hierarchically organized enzymes, which are very important in the initiation and execution of programmed cell death. The programmed cell death machinery, including the activation of caspases, is regulated by the integration of signals received from the extracellular environment and signals generated intracellularly. Once activated, caspases cleave their specific substrates in the cell, and eventually the cell disintegrates and it is removed from the environment.

In the framework of this study, the activation of seven different caspases will be investigated systematically, when extremely low frequency electromagnetic fields, which are thought to be an environmental hazard according to WHO, are applied to the HEK 293 cell line. The selected frequency will be 50 Hz, which is the power transmission line frequency in most parts of the world. Two different magnetic field strengths will be applied to HEK 293 cells, and two different exposure durations will be chosen. Caspase activity levels are to be measured at different time points after exposure.

According to the relevant scientific literature, the study presented here will be performed for the first time since the activities of seven different caspases have not been investigated, and compared in time series thus far.

3. MATERIALS

3.1. Cell Culture and Cell Viability

Cell line	: HEK 293 (ECACC, UK)
Fetal Bovine Serum (FBS)	: Heat-inactivated FBS (GibcoBRL, USA)
L-Glutamine	: 2 mM L-Glutamine (Sigma, USA)
Phosphate Buffered Saline	: 1X PBS, without (w/o) $MgCl_2$, w/o $CaCl_2$, (GibcoBRL, USA)
Non-essential Amino Acids	: 100X Non-essential amino acids (NEAA) (GibcoBRL, USA)
Penicillin/Streptomycine	: 100 mg/ml Penicillin/Streptomycine (p/s) (Sigma, USA)
Trypsin-EDTA	: 1X (GibcoBRL, USA)
Dimethylsulfoxide	: 100 per cent DMSO (Sigma, USA)
Minimal Essential Medium	: MEM with Earl's Salts, Glutamax-I (GibcoBRL, USA)
HEK 293 Medium	: 1 per cent NEAA, 1 per cent p/s, 1 per cent glutamine, 10 per cent FBS in MEM
Trypan Blue	: 0.4 per cent Trypan Blue (Sigma, USA)

Staurosporine : (Sigma, GERMANY)

3.2. Protein Quantification

Bovine Serum Albumine : Bovine Serum Albumine (BSA) Fraction V (Roche, GERMANY)

Bradford dye : Bradford dye concentrate (Bio-Rad, USA)

3.3. Caspase Activity Assay Kits

The Caspase Activity Colorimetric Assay Kits were purchased from BioVision, USA. Each kit contains reagents for cytoplasmic extraction, and a specific substrate for the respective caspase enzyme.

3.4. Chemicals

All solid and liquid chemicals used in this study were purchased from Merck (GERMANY) or Sigma (USA), unless stated otherwise in the text.

3.5. Equipment

Autoclave : Model MAC-601 (Eyela, JAPAN)

Balance : Electronic Balance VA124 (Gec Avery, UK)

Carbon dioxide tank : (Habaş, TURKEY)

Cell culture incubators : Thermo (Thermo Electron Corporation, USA), WTB (Binder, GERMANY)

Cell Culture Plastic Ware	: (Greiner, USA)
Centrifuges	: Centrifuge B5 (Braun Biotech International, GERMANY) Sigma 1-15 (Sigma, GERMANY)
Colorimeter	: Microplate Reader Model 680 (BioRad, USA)
Coverslips	: (Philip Harris, UK)
Deep Freezers	: -20°C (Bosch, GERMANY) -86°C ULT Freezer (ThermoForma, USA)
Gaussmeter	: R-F Surveymeter (Holaday Industries Inc., USA)
Haemocytometer	: (Fisher Scientific, UK)
Helmholtz coils	: (Eti Elektroteknik, TURKEY)
Incubator	: Binder APT Line Series (Binder, GERMANY)
Laminar Flow Cabinet	: (Esco, Singapore)
Magnetic Stirrer	: Hotplate Magnetic Stirrer, HS31 (Chiltern, UK)
Microscope	: CM110 Inverted Microscope (Prior, UK)
Refrigerators	: +4°C (Arçelik, TURKEY)

Transformers	: (Eti Elektroteknik, TURKEY)
Variac	: (Varsan, TURKEY)
Water Baths	: Thermomix. BU (Braun, GERMANY) Köttermann (Labortechnic, GERMANY)
Water Purification System	: Millipore SA 67120 (Millipore, FRANCE) Watech Water Technologies (TURKEY)

4. METHODS

4.1. Cell Culture

4.1.1. Maintenance of the HEK 293 Cell Line

The HEK 293 cell line was purchased from ECACC and maintained in its respective growth medium at a density of 2-5x100,000 cells/ml, in a humid 37°C incubator supplied with five per cent CO_2. The HEK 293 cells were grown in culture flasks in MEM supplemented with penicillin/streptomycin (100 unitsml^{-1}/100µgml^{-1}), glutamine (2 mM), 1X NEAA, and 10 per cent FBS. In order to split the adherent cells, cell monolayers were rinsed with sterile PBS and trypsinized in 500 µl, 0.05 per cent Trypsin/EDTA for three minutes at 37°C. Following dislocation of cells, trypsin was inhibited with 10 ml complete medium, and the cells were centrifuged at 1500 rpm for five minutes. Cell pellets were resuspended in complete medium and splitted 1/10.

4.1.2. Cell Counting

Cell suspensions were counted by using a haemocytometer. When the cover slip was placed onto the haemocytometer, five squares of one mm^2, each containing 16 squares become visible under the light microscope. The number of cells in each of the five squares were counted and divided into five, to obtain the average amount of cells present in one ml as a factor of 10^4.

4.1.3. Cell Storage

A flask of cells were collected by centrifugation at 1500 rpm for three minutes. The cell pellet was resuspended in five ml of cryopreservant, consisting of 10 per cent DMSO in FBS, and aliquoted into one ml fractions in cryovials. The cells in cryovials were cooled down to -20°C for an hour and then placed in the

-86°C freezer overnight, prior to long term storage at -196°C in liquid nitrogen tanks. When needed, cells were defrosted in a 37°C water bath for maximum 90 seconds and placed in flasks containing pre-warmed complete medium.

4.2. Application of ELF-EMFs to HEK 293 Cell Line

4.2.1. Establishment of ELF-EMF Source

Helmholtz coils were sterilized and placed into the cell culture incubator (Figure 4.1.). Each coil contains three mm wire wrapped around a circular insulator (100 times), and the coil diameter was 20 cm. The distance between the coils was 45 cm. The cables coming out of the coils were connected to a transformer (220-120 V) in series, which was connected in series to a second transformer (220-55 V). The second transformer was wired to the variac, and the variac was connected to the power line, of 220 V AC.

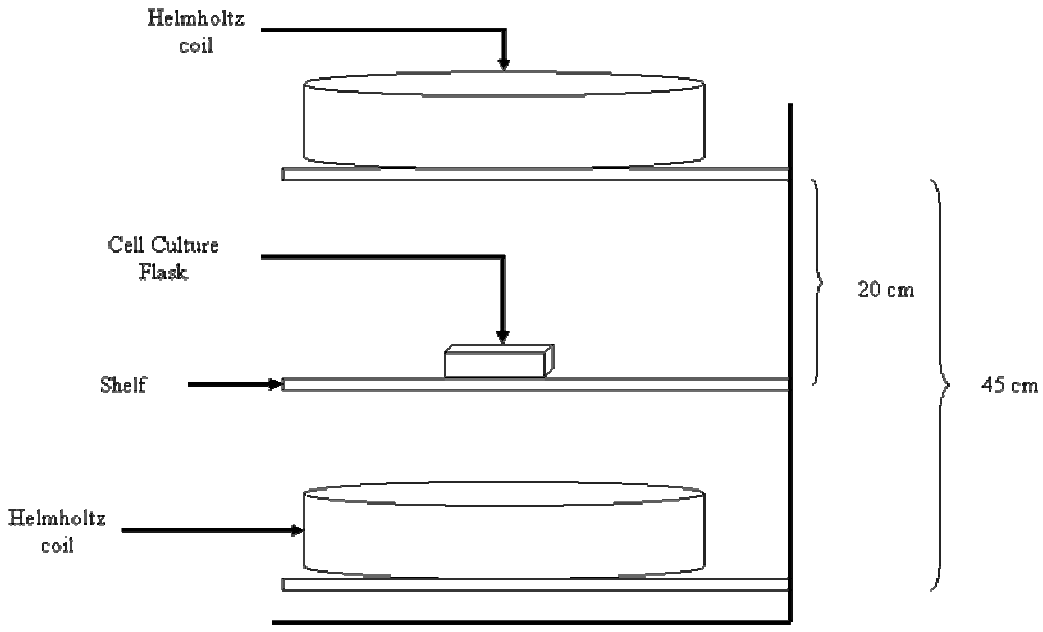

Figure 4.1. Schematic representation of the Helmholtz coils in the cell culture incubator

The frequency of the electromagnetic field produced between the Helmholtz coils was 50 Hz, because the system was directly connected to the power line. Different magnetic field strengths were generated by changing the electric current coming out of the variac, and by using one or both of the transformers in the system. The lower limit of the electromagnetic field, produced by the system, was 100 μT, when only the first transformer (220-120 V) was connected, whereas the limit was 25 μT, when the second transformer (220-55 V) was also wired to the system. The calibration of the system was done by using a gaussmeter, and a linear relationship between the current value and the electromagnetic field strength was achieved, as expected.

4.2.2. Exposure of ELF-EMF to HEK 293 Cells

HEK 293 cells were splitted into different flasks (25 cm^2) in a 1/15 ratio, and after 24 hours, these flasks were placed in an electromagnetic field with different exposure durations and different field strengths. Exposure durations were selected as four and eight hours, whereas electromagnetic field strengths were 25, and 100 μT.

4.3. Induction of Apoptosis by Using Staurosporine

In this study, apoptosis was induced in HEK 293 cells by using Staurosporine, which is a relatively non-selective, wide spectrum protein kinase inhibitor. Staurosporine was added to the cell culture medium with its final concentration of one μM, and the incubation time for inducing apoptosis was four hours at 37°C.

4.4. Cytoplasmic Extraction and Protein Quantification from the Cells

After ELF-EMF exposure or apoptosis induction by Staurosporine, cytoplasmic extractions were done according to the protocol of Caspase Colorimetric Assay Kits at different time points. Cells were dislocated by using 500 μl, 0.05 per cent Trypsin/EDTA after washing them with one ml of PBS. Dislocated cells (2-5x10^6 cells) were pelleted by centrifugation at 1500 rpm for four minutes. Pelleted cells were resuspended in 50 μl of chilled Cell Lysis Buffer, and they were incubated on ice for 10 minutes. After cell lysis, centrifugation was applied at 10,000xg for one minute, and

supernatant, which contains cytosolic extract, was transferred to a fresh tube. Cytoplasmic extracts should be kept on ice for immediate usage, or they should be kept at -86°C.

The cytoplasmic extracts were quantified by the Bradford Assay. Various concentrations of BSA (1.0-12.5 µg/ml) were used as a standard to calculate the concentrations of the extracts. BSA standards and 10 µl protein samples were mixed with Bradford dye concentrate such that the working concentration of the dye was reduced to 1/5. The samples were incubated at room temperature for 15 minutes and analyzed at 595 nm with the microplate reader. The required protein concentration for caspase activity assays is 100-200 µg.

4.5. Cell Viability and Caspase Activity Assays

After ELF-EMF exposure with two different exposure durations and three different magnetic field strengths, different time points were selected for the measurements of cell viability and caspase activity assays. Cell viability and caspase activity assays were also done after inducing apoptosis with Staurosporine.

4.5.1. Trypan Blue Exclusion Test

The Trypan Blue Exclusion method was used to detect the percentage of viable cells in a cell suspension. Trypan Blue is a negatively charged dye, which does not diffuse into the cell, unless the cell membrane is damaged. Therefore, cells excluding the dye are considered viable. In this assay, cells were harvested in PBS, and 20 µl of cell suspension was mixed with four µl of 0.4 per cent trypan blue dye. Then, the cells were incubated for three minutes and unstained cells were counted with a haemocytometer. Cell viability was determined by calculating the ratio of viable cells to the total number of cells.

4.5.2. Colorimetric Caspase Activity Assay

Cytoplasmic extracts were analyzed for Caspase-1, -2, -3, -6, -8, -9, and -10 by using the Caspase Colorimetric Assay Kits. The assay kits provide a simple and convenient means for assaying the activity of caspases. It is based on the spectrophotometric detection of the chromophore p-nitroanilide (pNA) after cleavage from the labeled substrate. Extracts were mixed with 50 µl of 2X Reaction Buffer, containing 10 mM dithiothreitol (DTT); 5 µl of the 4 mM substrate for the respective caspase was added and the resulting mixture was incubated at 37°C for two hours in a 96-well microtiter plate. After the incubation period, samples were read at 405 nm by using the microplate reader.

All experiments were performed as triplicates, and average values were used when drawing graphs.

5. RESULTS

5.1. Calibration of the Electromagnetic Field Generator

The system designed for producing extremely low frequency electromagnetic fields (ELF-EMFs), consists of two transformers, a variac, and two Helmholtz coils. Before starting the experiment, it is important to prove that the relation between the applied voltage to the Helmholtz coils and the magnetic field strength produced between them is linear. In order to investigate this relation, different voltage values were selected to be applied to the Helmholtz coils and the magnetic field strength generated, was measured by using a Gaussmeter, which is specific for the ELF-EMFs.

Table 5.1. Selected voltage values and their corresponding magnetic field strengths

Voltage (V)	Magnetic Field Strength (μT)
1	100
2	113
3	190
4	216
5	250
6	300
7	368
8	403
9	450
10	520
11	538
12	597
13	643
14	710
15	740
16	807
17	850
18	913
19	930
20	988
21	1030

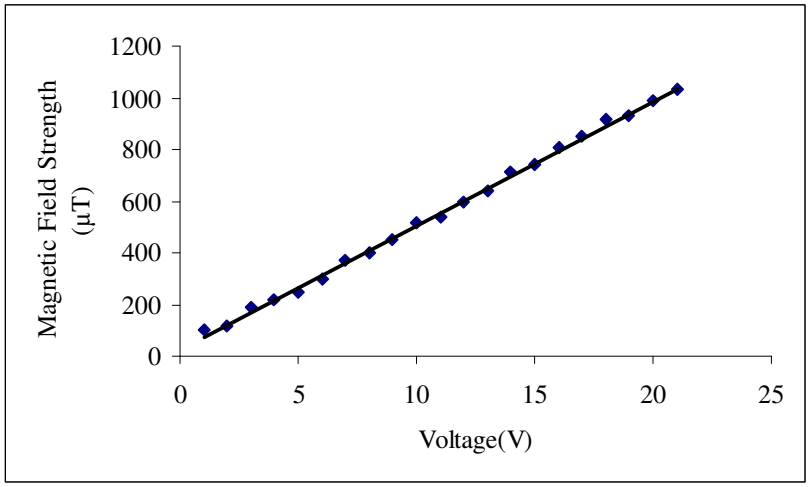

Figure 5.1. The linear relation between the applied voltage and the magnetic field strength generated by the Helmholtz coils

The linear relationship observed in Figure 5.1 has been taken as a proof that the system was working properly, when magnetic field strengths of 100 μT or values greater than 100 μT were selected. At this point only one transformer (220-120 V) was connected to the system. In order to reach magnetic field strengths less than 100 μT, a second transformer (220-55 V) was also connected to the system, and the calibration shown above was repeated.

Table 5.2. Selected voltage values and their corresponding magnetic field strengths, with the second transformer connected to the system

Voltage (V)	Magnetic Field Strength (μT)
1	25
2	35
3	50
4	55.9
5	67.5
6	80
7	97
8	105.6

The relationship between the voltage values selected and their corresponding magnetic field strengths had again a linear relation, being the proof that the system

with two transformers was working properly when the magnetic field strengths of less than 100 μT were aimed.

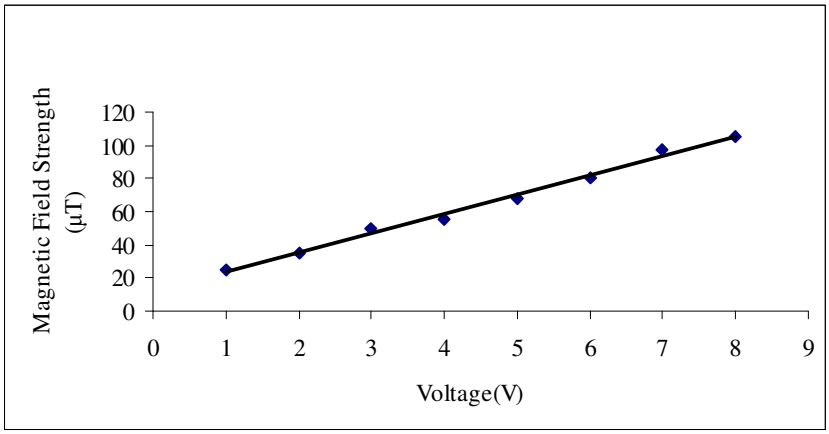

Figure 5.2. The linear relationship between the applied voltage and the magnetic field strength generated when less than 100 μT was aimed

5.2. Measurement of Caspase Activities after the Application of ELF-EMF

After calibration of the established experimental system, two different magnetic field strengths (25 and 100 μT) were applied to the HEK293 cells with two different exposure durations (four and eight hours). After applying the ELF-EMFs, activities of seven different caspases (Caspase-1, -2, -3, -6, -8, -9 and -10) were measured colorimetrically at the end of the incubation time points. All caspase activity measurements were performed nine times, and each data point in the activity graphs represents the average values of these nine measurements.

The data generated were interpreted from two different perspectives. First, keeping the exposure time fixed, data were compared with respect to different magnetic field strengths for each caspase, and results were also compared with data from sham-exposed cells. The second perspective was that with fixed magnetic field strengths, data for each caspase were compared with respect to different exposure durations, and again the results were compared with the data derived from sham-exposed cells.

In order to compare the increase of caspase activities after ELF-EMF exposure with the staurosporine-induced increase of caspase activities, data from four-hour incubation time of two different magnetic field strengths were compared with the data produced from four-hour incubation time of staurosporine-induced HEK 293 cells.

5.2.1. Measurement of Caspase Activities with Fixed Exposure Time

In order to compare the caspase activities at two different magnetic field strengths, data derived from each caspase at 25 μT were compared with data generated at 100 μT for the same caspase, when exposure durations were fixed.

In Figure 5.3 data for caspase-1 are presented, when 25 and 100 μT ELF-EMFs were applied for four-hour exposure duration (Table A.1).

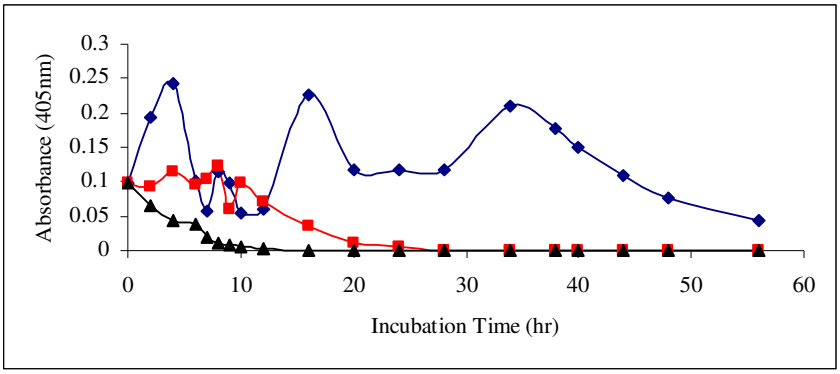

Figure 5.3. Change of caspase-1 activity with respect to time.
blue curve: 100 μT, red curve: 25 μT, black curve: sham-exposed cells

As shown in Figure 5.3, when 100 μT was applied to the HEK 293 cells for four-hour exposure duration, caspase-1 activity began to oscillate with respect to incubation time. It gave a maximum at four-hour incubation time, and then it gave three more peaks at eigth, 16 and 34-hour incubation times. After the last peak it diminished continuously. On the other hand, when 25 μT was applied for four-hour exposure duration, caspase-1 activity gave three peaks at four, eight and 10-hour incubation times. Moreover, its oscillation amplitude was very small compared with that of the

100 μT data, and the activity of caspase-1 converged to the activity derived from sham-exposed cells at 28-hour incubation time.

Data for caspase-2 activity were presented in Figure 5.4, and exposure conditions were the same as for the caspase-1, mentioned above (Table A.2).

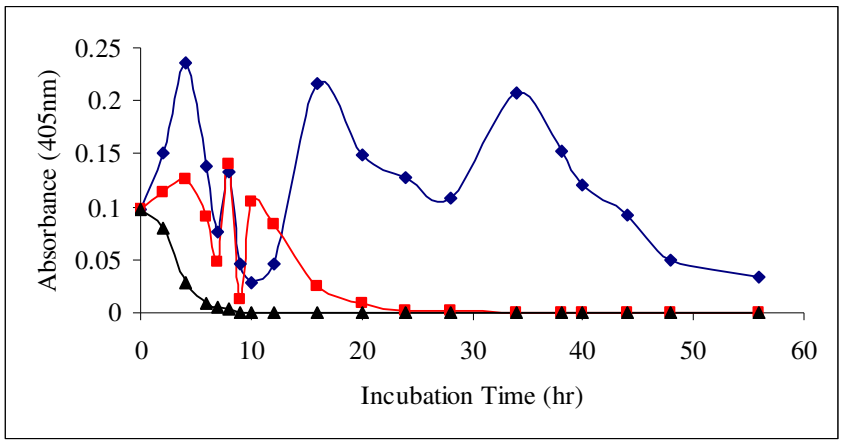

Figure 5.4. Change of caspase-2 activity with respect to time.
blue curve: 100 μT, red curve: 25 μT, black curve: sham-exposed cells

When the 100 μT magnetic field was applied for four hours, caspase-2 activity revealed an oscillation pattern, which was very similar to that of the caspase-1. Caspase-2 activity showed a maximum at four-hour incubation time, and it also gave three additional peaks at eight, 16 and 34-hour incubation times. Then, it approached gradually to zero. When 25 μT was applied for four-hour exposure duration, caspase-2 activity showed an oscillatory pattern again, but it gave three peaks. The second peak, which corresponds to eight-hour incubation, was the maximum. However, all peaks were smaller than those at 100 μT, and the caspase-2 activity at 25 μT approached to zero at 24-hour incubation time.

In Figure 5.5 and Table A.3, activity of caspase-3 is revealed, and the exposure conditions were the same.

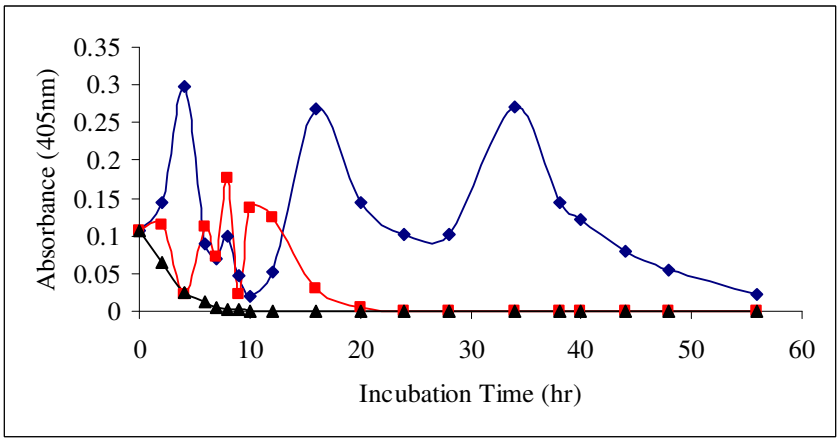

Figure 5.5. Change of caspase-3 activity with respect to time.
blue curve: 100 μT, red curve: 25 μT, black curve: sham-exposed cells

As shown in Figure 5.5, the change in caspase-3 activity was very similar to the changes in caspase-1 and caspase-2 activities. The characteristic four peaks at 100 μT were observed at the same incubation periods, and after the last peak, the caspase-3 activity started to decrease continuously. The same interpretation can be made for the 25 μT exposure. It gave peaks, which were smaller than peaks for 100 μT exposure, and the location of peaks seemed to shift. The caspase-3 activity converged to zero at 24-hour incubation time again.

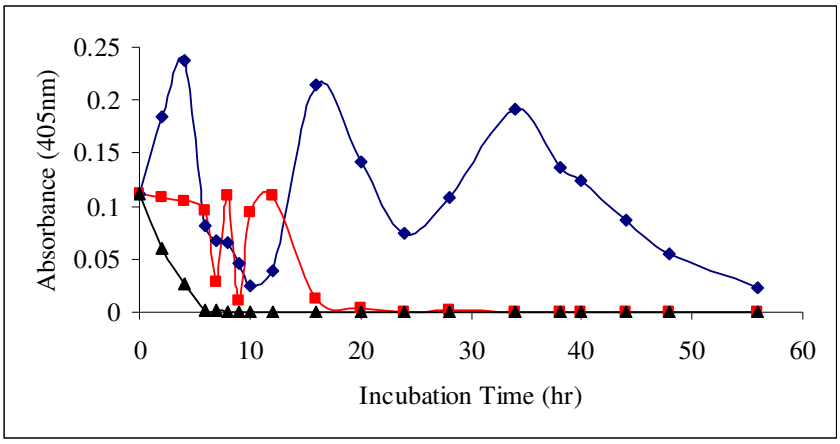

Figure 5.6. Change of caspase-6 activity with respect to time.
blue curve: 100 μT, red curve: 25 μT, black curve: sham-exposed cells

The same general pattern was observed for caspase-6 activity at 100 and 25 μT exposures, respectively (Figure 5.6 and Table A.4). For 25 μT exposure, there were two peaks at eight and 12-hour incubation times, whereas around four-hour incubation a plateau was observed.

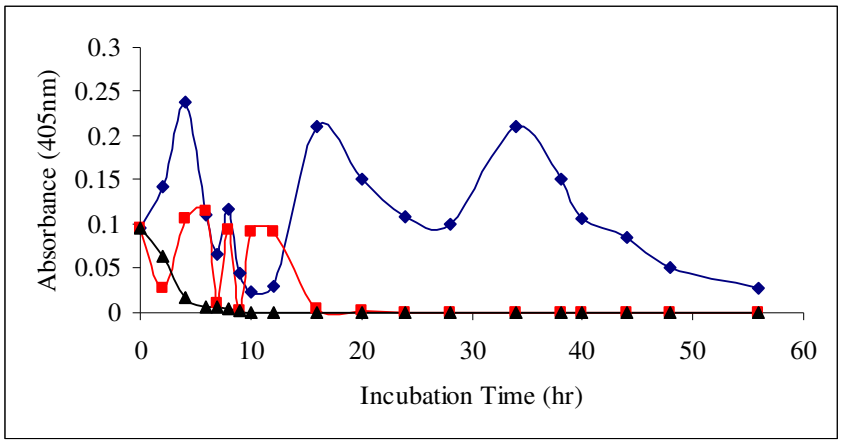

Figure 5.7. Change of caspase-8 activity with respect to time. blue curve: 100 μT, red curve: 25 μT, black curve: sham-exposed cells

Figure 5.7 and Table A.5 show the data for caspase-8 activities when 25 and 100 μT were applied for four-hour exposure duration. An oscillatory pattern was observed especially for the 100 μT exposure. For the 25 μT exposure, there were three peaks at six, eight and 10 hour-incubation times. Caspase-3 activity approached to zero at 16-hour incubation, when 25 μT was applied.

When these two magnetic field strengths were applied to caspase-9 activity, four peaks were also found at 100 μT. On the other hand, at 25 μT, caspase-9 activity was observed to be very small, compared with the previous caspase activities at the same magnetic field strength (Figure 5.8 and Table A.6).

When caspase-10 activity was examined for 100 μT exposure, the pattern observed was very similar to those of the previous caspases. However, the situation was found to be different, when 25 μT was applied. First of all, peaks produced were larger than the peaks generated by the other caspases. The peak at eigth-hour incubation time was at maximum, and it was even bigger than the maximum value of

100 μT exposure. Caspase-10 activity for 25 μT exposure converged to zero at 28-hour incubation time (Figure 5.9 and Table A.7).

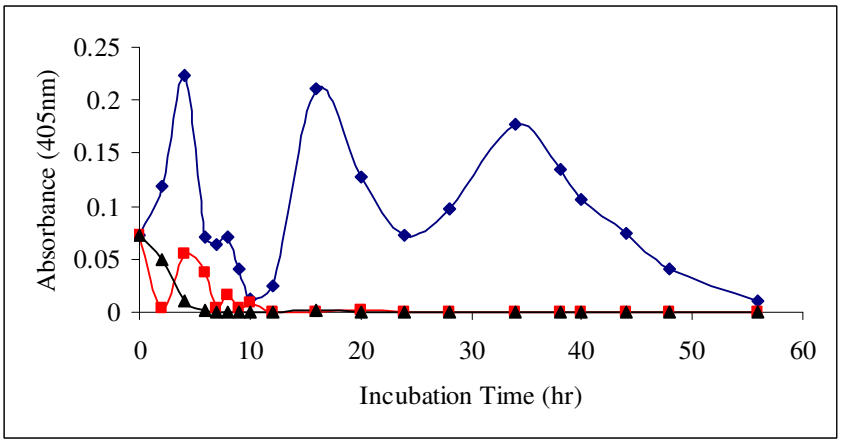

Figure 5.8. Change of caspase-9 activity with respect to time. blue curve: 100 μT, red curve: 25 μT, black curve: sham-exposed cells

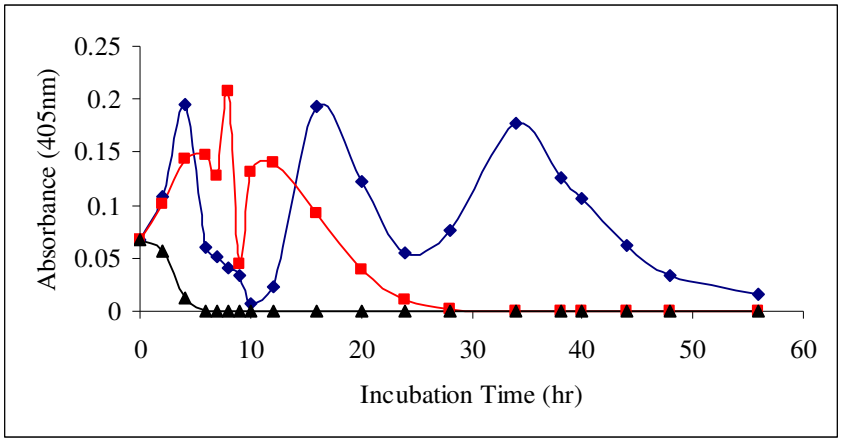

Figure 5.9. Change of caspase-10 activity with respect to time. blue curve: 100 μT, red curve: 25 μT, black curve: sham-exposed cells

The same treatment was made to HEK 293 cells, namely two different magnetic field strengths were applied, but this time exposure duration was selected as eight hours.

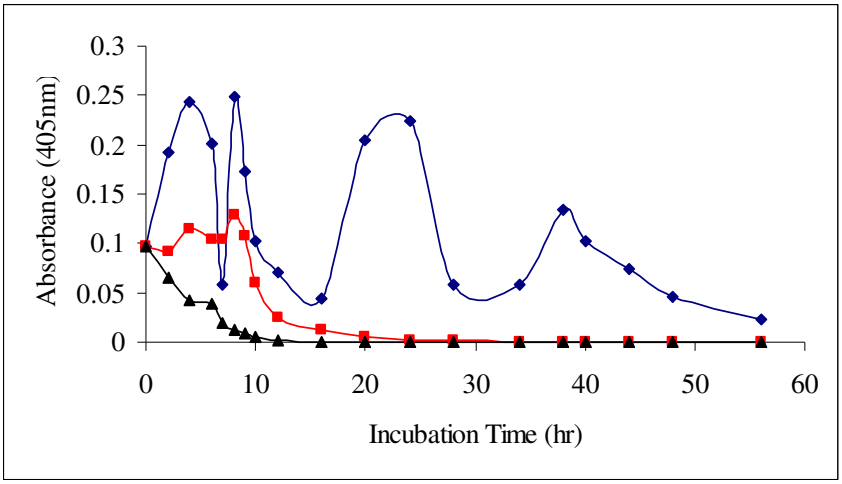

Figure 5.10. Change of caspase-1 activity with respect to time.
blue curve: 100 µT, red curve: 25 µT, black curve: sham-exposed cells

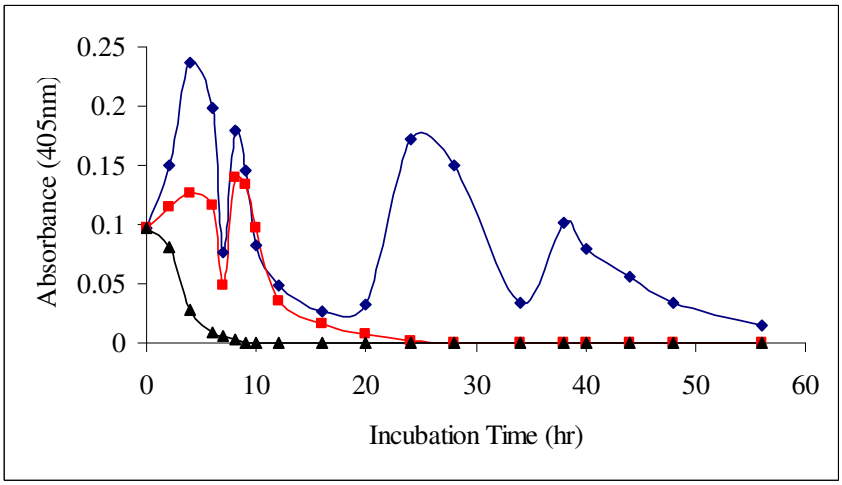

Figure 5.11. Change of caspase-2 activity with respect to time.
blue curve: 100 µT, red curve: 25 µT, black curve: sham-exposed cells

As can be seen from Figure 5.10 to Figure 5.16 (from Table A.8 to Table A.14), patterns of the curves derived from 100 µT magnetic field strength were similar to the ones with four hours exposure. Moreover, when 25 µT was applied, the patterns observed were also similar to curves for 25 µT (four hours exposure).

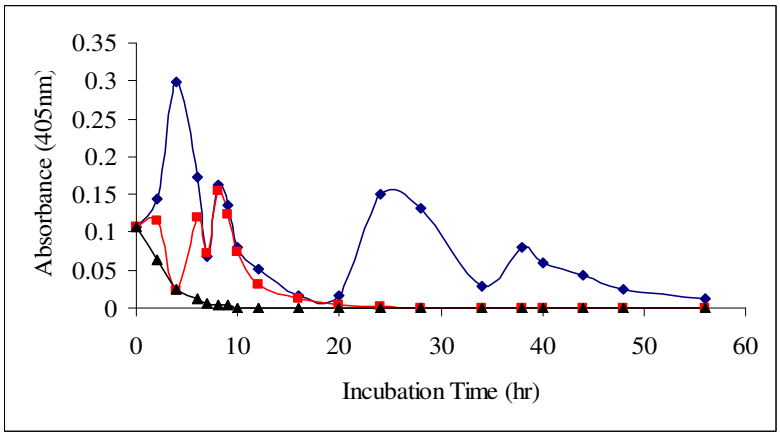

Figure 5.12. Change of caspase-3 activity with respect to time.
blue curve: 100 μT, red curve: 25 μT, black curve: sham-exposed cells

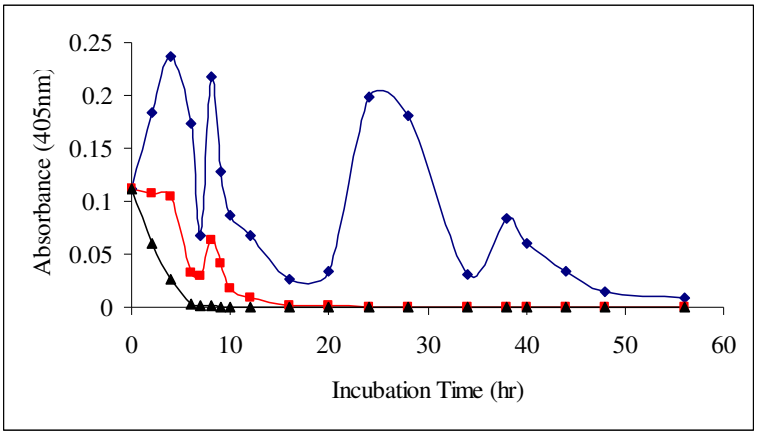

Figure 5.13. Change of caspase-6 activity with respect to time.
blue curve: 100 μT, red curve: 25 μT, black curve: sham-exposed cells

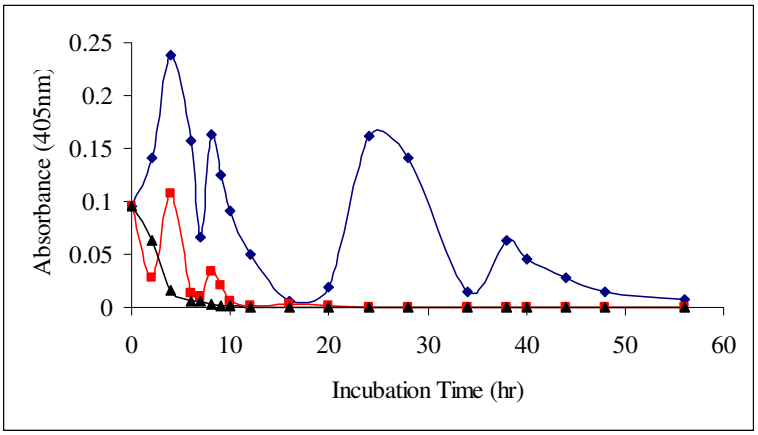

Figure 5.14. Change of caspase-8 activity with respect to time.
blue curve: 100 μT, red curve: 25 μT, black curve: sham-exposed cells

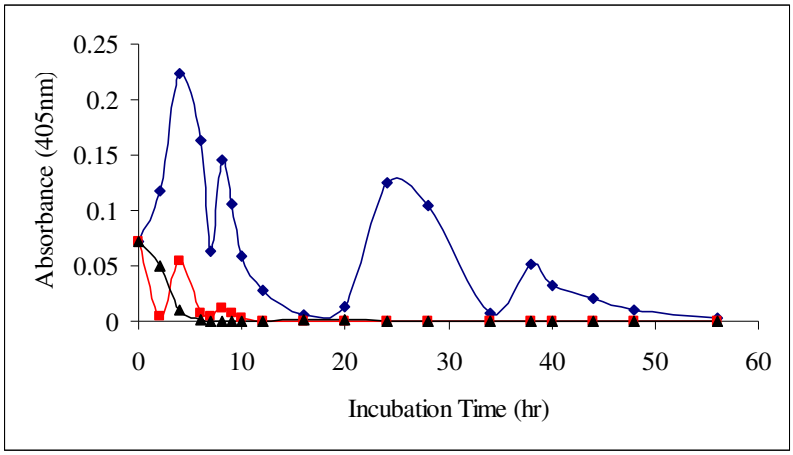

Figure 5.15. Change of caspase-9 activity with respect to time.
blue curve: 100 μT, red curve: 25 μT, black curve: sham-exposed cells

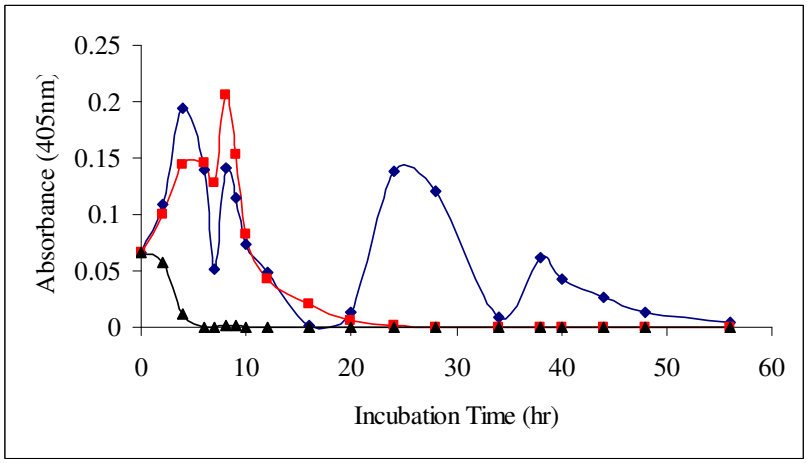

Figure 5.16. Change of caspase-10 activity with respect to time.
blue curve: 100 μT, red curve: 25 μT, black curve: sham-exposed cells

5.2.2. Measurement of Caspase Activities with Fixed Magnetic Field Strengths

In order to elucidate the changes in caspase activities with respect to exposure duration, applied magnetic field strengths were kept constant and activity changes were observed for four and eight hours exposure durations for each caspase.

In Figure 5.17 changes in caspase-1 activity are presented when 100 μT magnetic field was applied to HEK 293 cells for two different exposure durations(Table A.15).

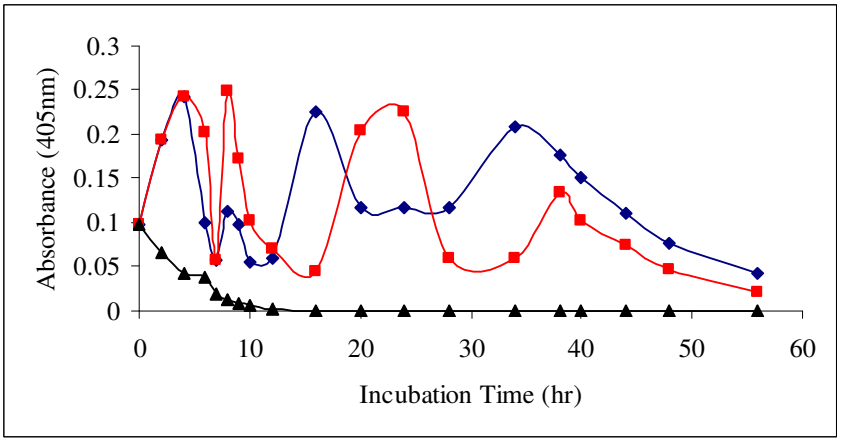

Figure 5.17. Change of caspase-1 activity at 100 µT with respect to time.
blue curve: four hours, red curve: eight hours, black curve: sham-exposed cells

For 100 µT caspase-1 activities for four and eight-hour exposure durations seemed to be parallel until 12-hour incubation time. After this point an activity shift with respect to time was observed until 40-hour incubation time. Then these two curves began to decrease continuously. In addition to this difference, the maximum value was reached at eight-hour incubation, when the exposure duration was eight hours.

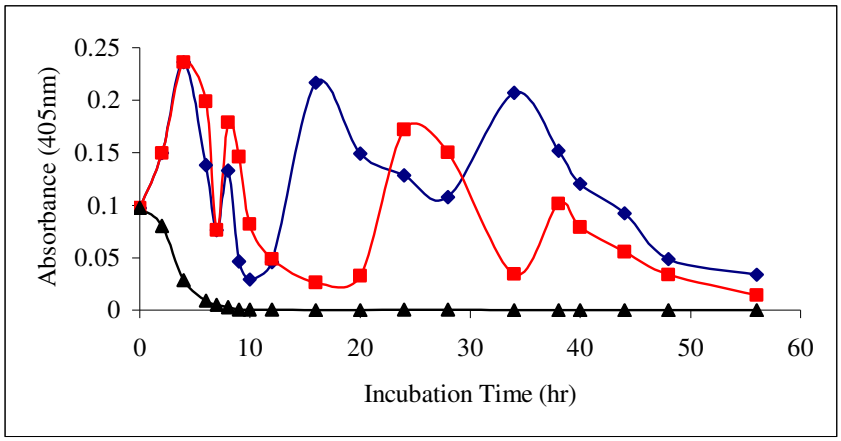

Figure 5.18. Change of caspase-2 activity at 100 µT with respect to time.
blue curve: four hours, red curve: eight hours, black curve: sham-exposed cells

When 100 µT was applied to HEK 293 cells, caspase-2 activity showed a very similar pattern with caspase-1 at four and eight hours exposure durations. The only

difference found was that the maximum values for the two exposure durations were at four-hour incubation time (Figure 5.18 and Table A.16).

In Figure 5.19 and Table A. 17, pattern was not different from patterns of caspase-1 and caspase-2. Unlike caspase-1, it gave maximum values at the same incubation points (four-hour incubation).

Figure 5.20 reveals the changes in caspase-6 activities at 100 μT for the same exposure durations (Table A.18). Maximum values were again at the same incubation points, whereas the second peak for eight-hour incubation was larger than the corresponding peaks for caspase-3 and caspase-6.

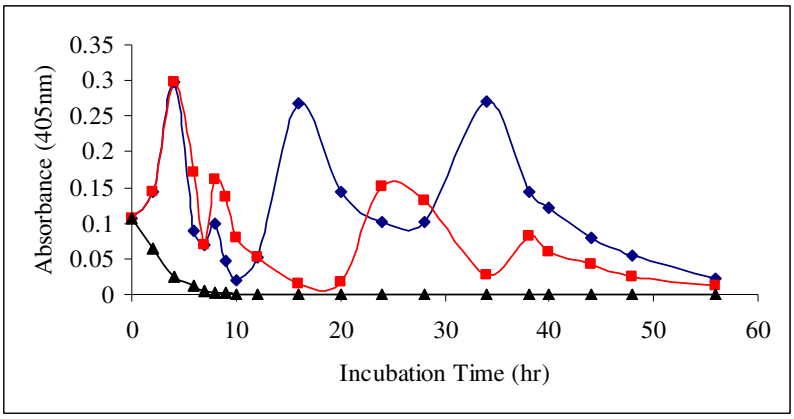

Figure 5.19. Change of caspase-3 activity at 100 μT with respect to time.
blue curve: four hours, red curve: eight hours, black curve: sham-exposed cells

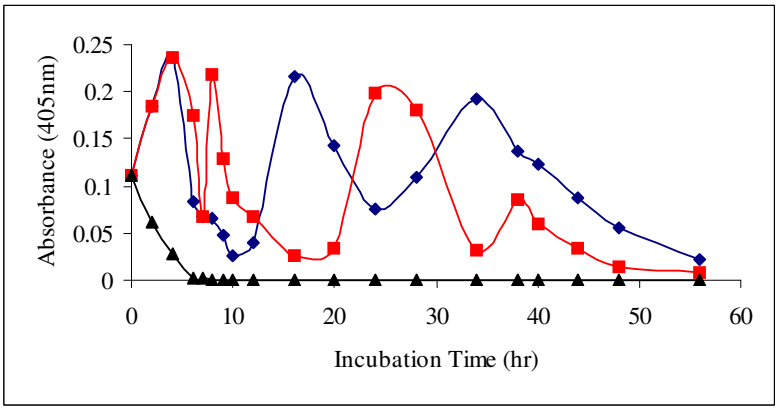

Figure 5.20. Change of caspase-6 activity at 100 μT with respect to time.
blue curve: four hours, red curve: eight hours, black curve: sham-exposed cells

The activity changes in caspase-8 were also similar to the previous caspases (Figure 5.21 and Table A.19).

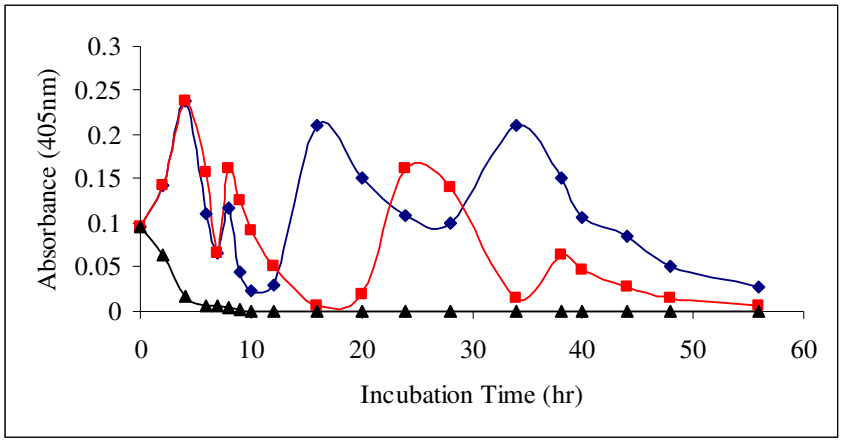

Figure 5.21. Change of caspase-8 activity at 100 μT with respect to time. blue curve: four hours, red curve: eight hours, black curve: sham-exposed cells

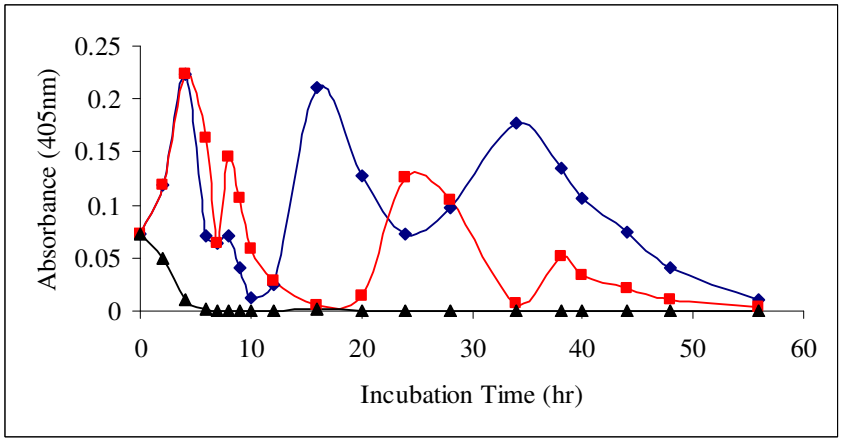

Figure 5.22. Change of caspase-9 activity at 100 μT with respect to time. blue curve: four hours, red curve: eight hours, black curve: sham-exposed cells

Caspase-9 and caspase-10 activities also gave similar patterns (Figure 5.22 and Figure 5.23; Table A.20 and Table A.21, respectively).

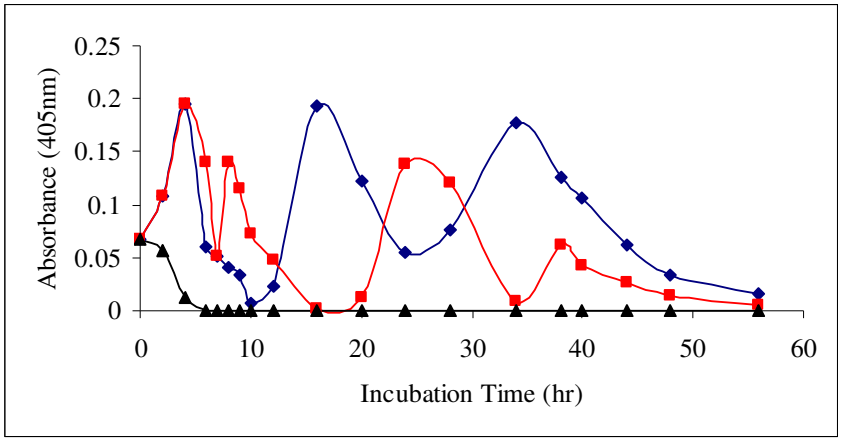

Figure 5.23. Change of caspase-10 activity at 100 µT with respect to time.
blue curve: four hours, red curve: eight hours, black curve: sham-exposed cells

The same analyses were performed by applying a 25 µT magnetic field for the two exposure durations.

Figure 5.24 and Table A.22 show the change of caspase-1 activity at 25 µT for four and eight-hour exposure durations.

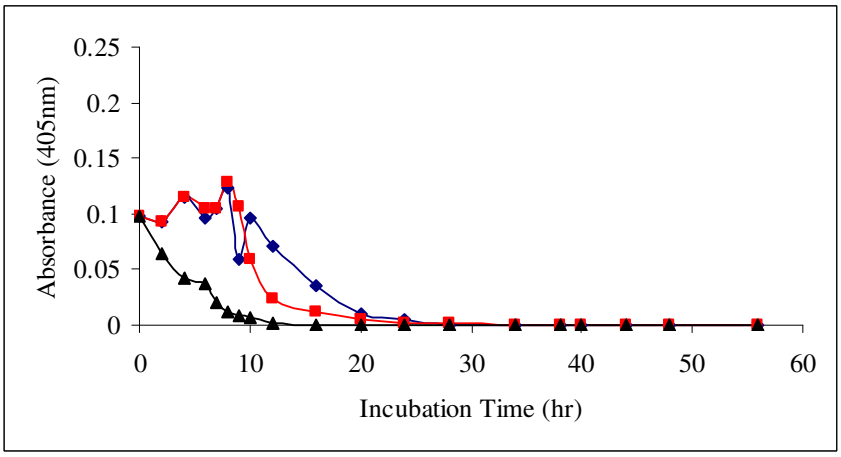

Figure 5.24. Change of caspase-1 activity at 25 µT with respect to time.
blue curve: four hours, red curve: eight hours, black curve: sham-exposed cells

Caspase-1 activities for the two exposure time points showed a similar pattern. Peaks were very small and the maximum values were at eight-hour incubation. In

addition, there was a second peak at 10-hour incubation when the exposure time was four hours.

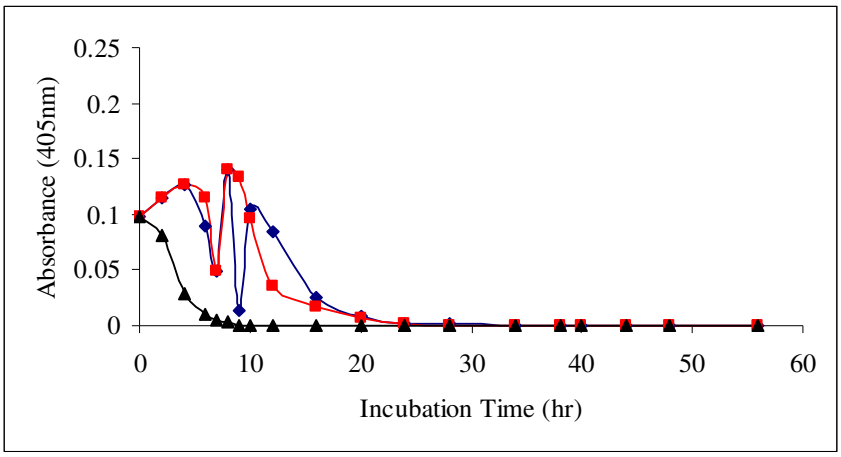

Figure 5.25. Change of caspase-2 activity at 25 μT with respect to time. blue curve: four hours, red curve: eight hours, black curve: sham-exposed cells

In Figure 5.25 (Table A.23), curves for the two exposure times were again similar to each other and to the curves of caspase-1.

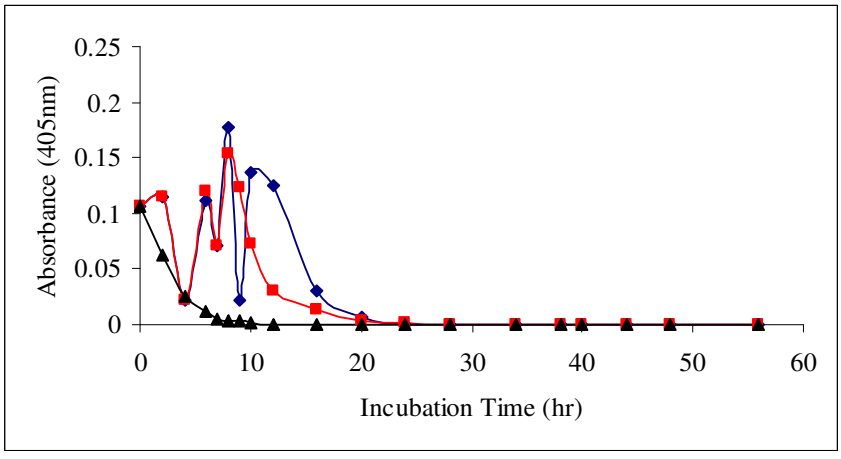

Figure 5.26. Change of caspase-3 activity at 25 μT with respect to time. blue curve: four hours, red curve: eight hours, black curve: sham-exposed cells

Figure 5.26 reveals the same pattern for caspase-3, however, the maximum value of four-hour exposure was greater than the eight-hour-exposure at eight-hour incubation time (Table A.24).

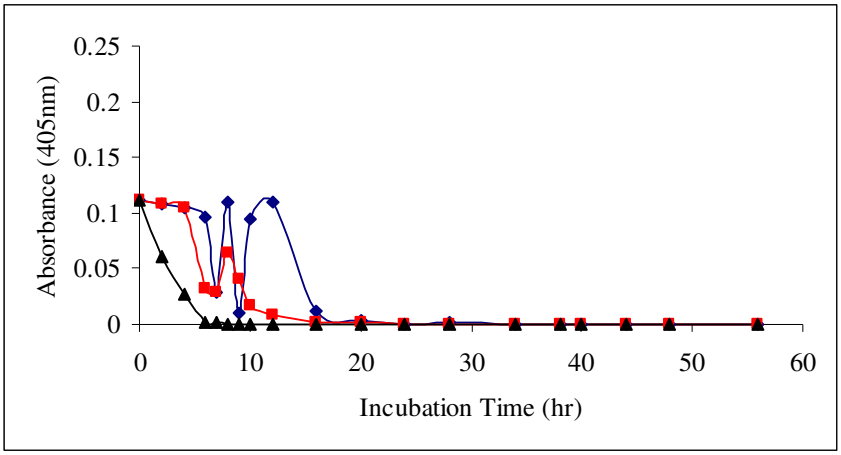

Figure 5.27. Change of caspase-6 activity at 25 μT with respect to time.
blue curve: four hours, red curve: eight hours, black curve: sham-exposed cells

The changes in caspase-6 activities were found to be similar with the previous caspases (Figure 5.27 and Table A.25).

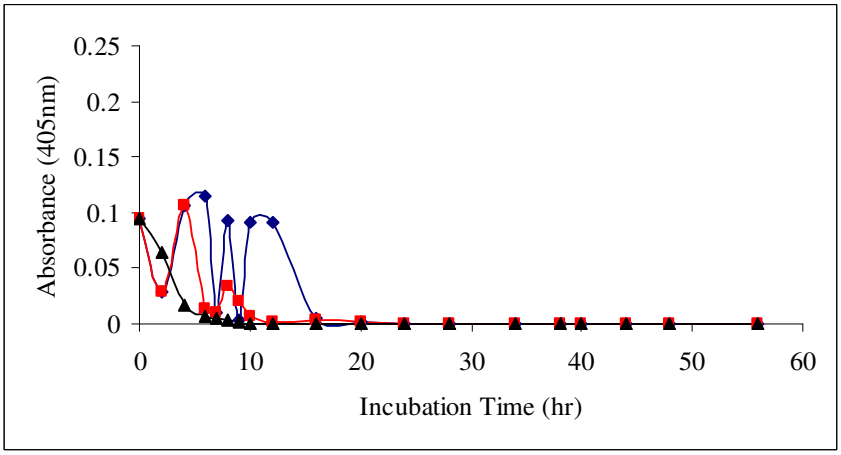

Figure 5.28. Change of caspase-8 activity at 25 μT with respect to time.
blue curve: four hours, red curve: eight hours, black curve: sham-exposed cells

Caspase-8 revealed a similar pattern to the other caspases (Figure 5.28 and Table A.26). On the other hand, data for caspase-9 showed that the enzyme activities were comparable with negative controls from the beginning, and they immediately dropped to zero at around eight-hour incubation (Figure 5.29 and Table A.27).

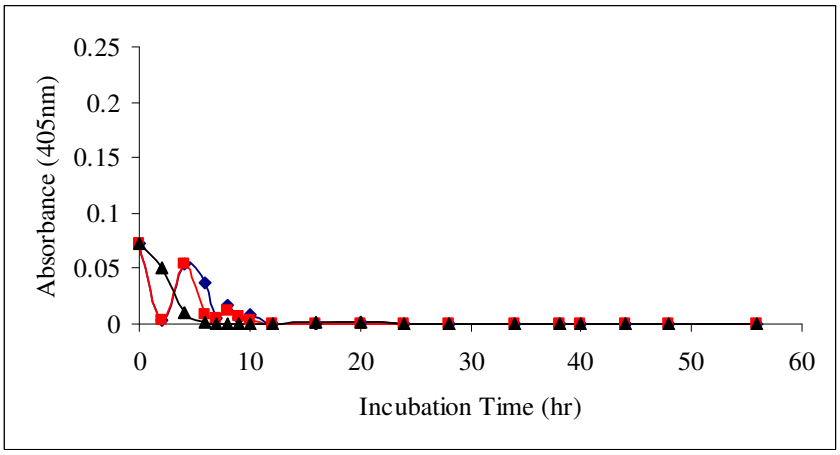

Figure 5.29. Change of caspase-9 activity at 25 μT with respect to time. blue curve: four hours, red curve: eight hours, black curve: sham-exposed cells

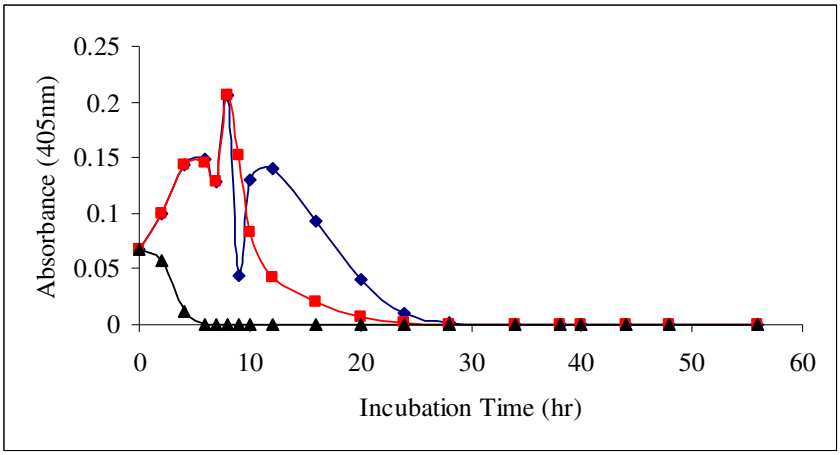

Figure 5.30. Change of caspase-10 activity at 25 μT with respect to time. blue curve: four hours, red curve: eight hours, black curve: sham-exposed cells

The maximum values for caspase-10 for the two exposure durations were matched at eight-hour incubation, and the general pattern of the curves were similar to the previous ones (Figure 5.30 and Table A.28).

5.2.3. Comparison of Maximum Values of Each Caspase Activity

In order to compare the enzyme activity levels from ELF-EMF exposed HEK 293 cells with those of staurosporine treated HEK 293 cells, four hours exposure data

were taken from 25 and 100 μT applied cells, and they were compared with the data generated from one μM, four hours staurosporine treated cells.

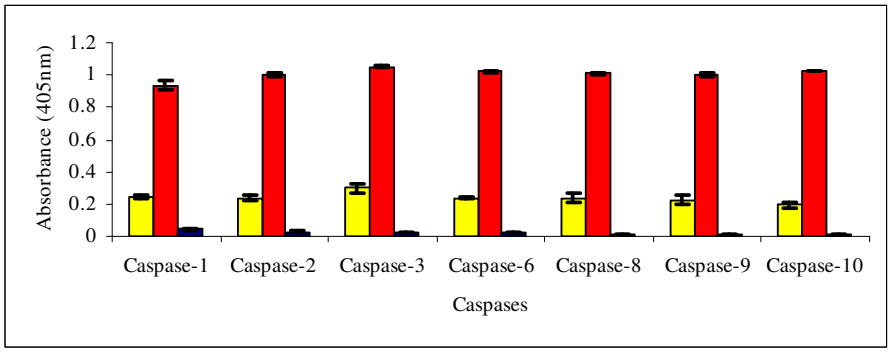

Figure 5.31. Comparisons of caspases; yellow columns: 100 μT exposed, red columns: staurosporine treated and blue columns: sham exposed cells

As shown in Figure 5.31, caspase activities were found to be increased with respect to data derived from sham-exposed cells, after 100 μT EMF was applied for four hours. However, when data from ELF-EMF exposed cells were compared with staurosporine treated cells, it was very obvious that the activity increases in caspases after ELF-EMF exposure were comparably small (Table A.29, Table A.30 and Table A.32).

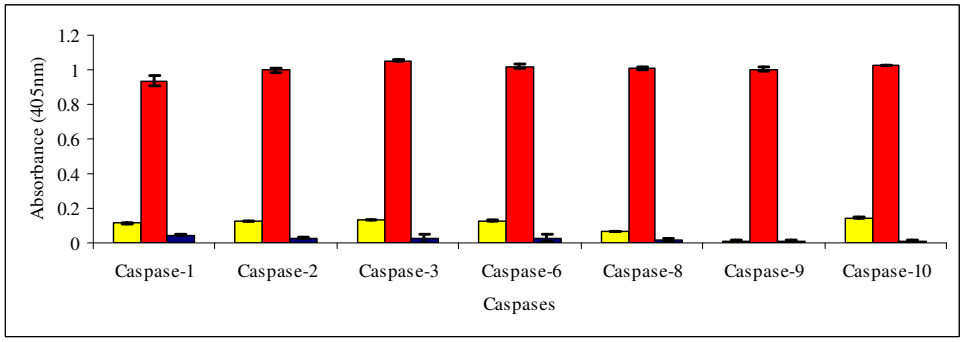

Figure 5.32. Comparisons of caspases; yellow columns: 25 μT exposed, red columns: staurosporine treated and blue columns: sham-exposed cells

Figure 5.32 shows that increases in caspase activities at 25 μT were less than those at 100 μT, and they were still greater than the activities produced by sham-exposed cells except caspase-9 (Table A.29, Table A.31 and Table A.32).

5.3. Measurement of Cell Viability after the Application of ELF-EMF

In addition to the activity measurements of seven different caspases, a cell viability assay was performed for each exposure duration, and magnetic field strength value, and the same set of time points were used for this measurement. The graphs of cell viability assays were grouped according to magnetic field strengths. In each graph, cell viability results derived from induction of apoptosis by staurosporine, and results for sham-exposed cells were included for comparison.

According to Figure 5.33 and Figure 5.34, it is very likely that when a 100 μT magnetic field was applied to the HEK293 cells for four and eight hours durations, there is not a significant difference between the exposed and sham-exposed cells with the given incubation time points (Table A.33, and Table A.34). In addition, there is a big difference between ELF-EMF-exposed cells and staurosporine-treated cells in terms of cell viability.

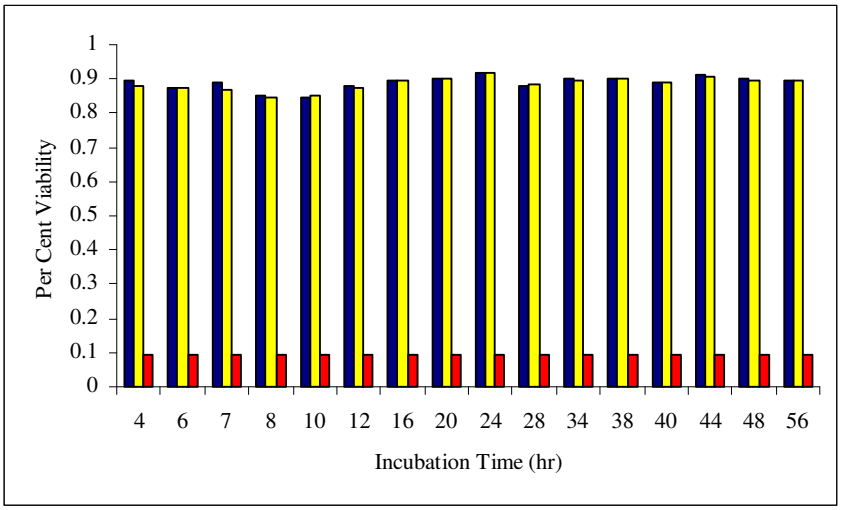

Figure 5.33 Results of Trypan Blue Exclusion Test, when 100 μT ELF-EMF was applied to HEK293 cells for four hours, blue columns: Results of sham-exposed HEK293 cells, yellow columns:ELF-EMF-exposed HEK293 cells, red columns: Staurosporine-treated HEK293 cells

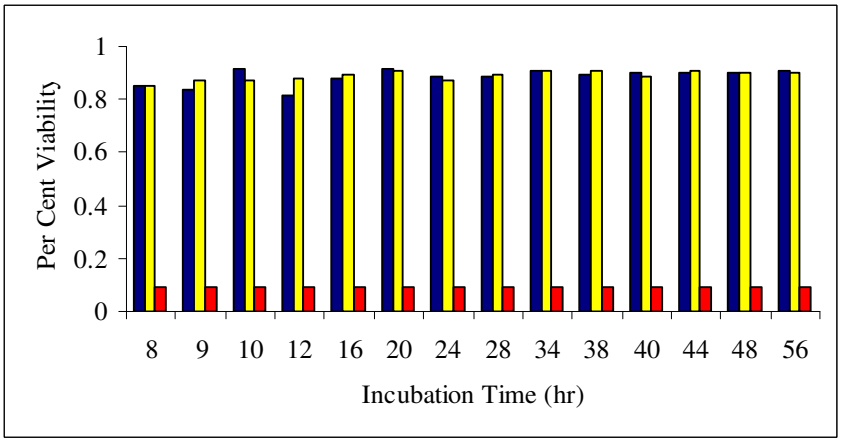

Figure 5.34 Results of Trypan Blue Exclusion Test, when 100 μT ELF-EMF was applied to HEK293 cells for eight hours; blue columns: Results of sham-exposed HEK293 cells, yellow columns:ELF-EMF-exposed HEK293 cells, red columns: Staurosporine-treated HEK293 cells

In the second experiment, for the measurement of cell viability, a 25 μT magnetic field was applied to the HEK293 cells for four and eight hours exposure durations, and Trypan Blue Exclusion test was performed for each incubation time point (Figure 5.35, Table A.35, and Figure 5.36, Table A.36).

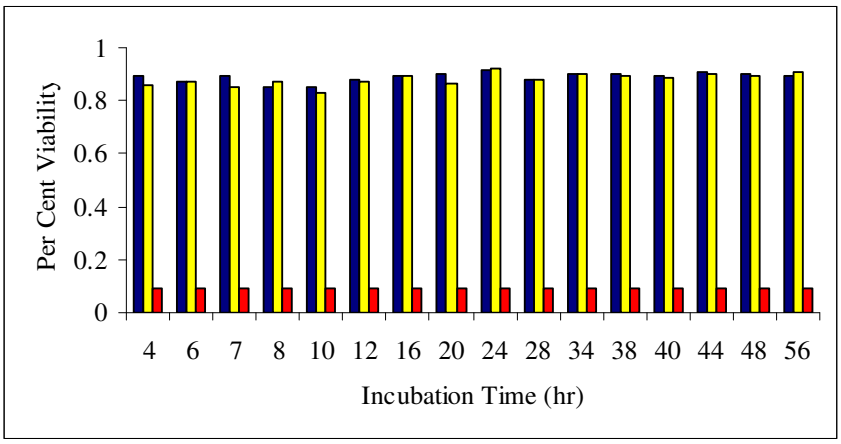

Figure 5.35 Results of Trypan Blue Exclusion Test, when 25 μT ELF-EMF was applied to HEK293 cells for four hours, blue columns: Results of sham-exposed HEK293 cells, yellow columns:ELF-EMF-exposed HEK293 cells, red columns: Staurosporine-induced HEK293 cells

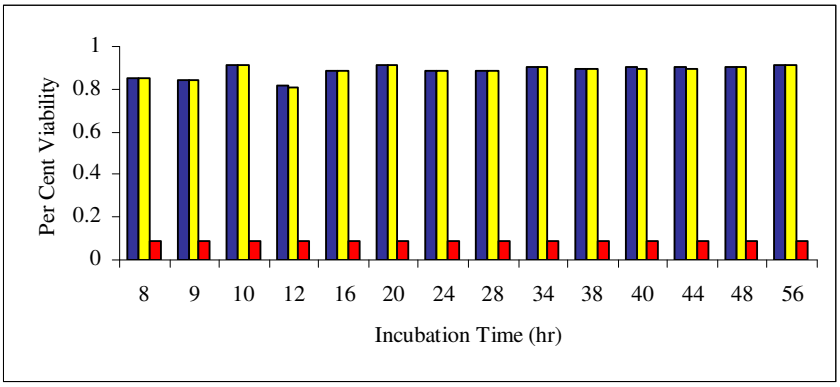

Figure 5.36 Results of Trypan Blue Exclusion Test, when 25 μT ELF-EMF was applied to HEK293 cells for eight hours, blue columns: Results of sham-exposed HEK293 cells, yellow columns:ELF-EMF-exposed HEK293 cells, red columns: Staurosporine-induced HEK293 cells

6. DISCUSSION

6.1. Effects of ELF-EMFs on Living Systems

There is a growing number of interest in possible health effects associated with exposure to ELF-EMFs. There has been more concern on this topic as a result of epidemiological studies. These suggest a possible, but controversial link between exposure to ELF-EMFs and an increased incidence of some cancers in both children and adults, especially leukemia and nervous system tumors. The controversy has been tried to be solved by laboratory studies both in vitro and in vivo. Animal studies revealed that no definite conclusion can be drawn on the potential health hazard associated with ELF-EMFs. Although some studies show teratogenic and/or carcinogenic effects of ELF-EMFs, there are others concluding that no direct relationship exists between exposure to ELF-EMFs and teratogenesis or carcinogenesis.

The possible effects of ELF-EMFs have also been studied by using cell culture models. Different cellular targets related to carcinogenesis, such as genotoxic effects, gene expression, intracellular Ca^{+2} concentration and transport, and cell proliferation, have been investigated in different cell culture systems. In some of the cell culture studies, ELF-EMFs do not seem to exert any direct genotoxic effect, but they may participate in carcinogenesis by influencing the cell proliferation, probably interfering with signal transduction pathways of the cells. There are many reports on the effects of ELF-EMFs on neuronal cells in vitro, although results are not conclusive and sometimes even conflicting. Some studies reported that exposure of a rat pheocromocytoma cell line (PC 12 cells) to ELF-EMFs can either increase or decrease neurite outgrowth, depending on the subset of PC 12 cells used. Changes in neurite outgrowth but not in cell division, depending on field strength and culture conditions, were reported in the same cellular model.

In contrast to the multitude of the studies concerning the effects of ELF-EMFs on carcinogenesis, there is a very limited number of studies, which were devoted to investigate the possible effects of ELF-EMFs on other endpoints of crucial interest for cancer risk, namely apoptosis. As the studies about the possible role of ELF-EMFs on carcinogenesis are conflicting, results of the investigations about the possible role of ELF-EMFs on apoptosis are controversial. In some studies, cellular morphologies which are the indicators of apoptosis, have been observed after the exposure of ELF-EMFs, and other studies also reveal that activities of some caspases have been found to be elevated. However, still other studies concerning the possible role of ELF-EMFs on apoptosis show that exposure to ELF-EMFs suppress the triggering of apoptotic mechanisms, such as caspase activation, moreover they can increase the proliferative potential of the cell.

6.2. Behaviours of Caspases After the Application of 50 Hz ELF-EMFs

In the framework of this thesis, behaviours of seven different caspases were investigated in the presence of two different magnetic field strengths (25 and 100 μT) for four hours exposure (Figure 5.3, Figure 5.4, Figure 5.5, Figure 5.6, Figure 5.7, Figure 5.8, and Figure 5.9). The common pattern seen in all of them was the oscillation of enzyme activities from the beginning. At 100 μT, caspases gave four peaks at four, eight, 16 and 34-hour incubation periods, and the largest of these peaks was at four-hour incubation time for every caspase. The second peaks, which were the smallest of all, were always at eight-hour incubation. For caspase-9, this second peak can be seen as a shoulder, while in caspase-10 there was no peak at all. Another common theme for all caspases after 100 μT, four hours exposure was the gradual but continuous decrease of the enzyme activities after the last peak (at 34-hour incubation).

This oscillatory behavior can also be seen when 25 μT magnetic field was applied for four hours, but the behaviors of the enzymes were different in a certain extent. The location and the number of the peaks at 25 μT exposure were quite variable, but the activity periods of all caspases seemed to be shorter than those exposed to 100 μT. After 24-hour incubation time point, the activities of all caspases were zero. One important exception was caspase-10. The activity reached by caspase-

10 at 25 μT was even greater than the maximum value of the same enzyme when 100 μT was applied.

When the exposure time was extended to eight hours, the general pattern of oscillation remained, but with some differences. There were four peaks at 100 μT, and eight hours exposure, and the largest one was at four-hour incubation time except for caspase-1, whose maximum was at eight-hour incubation time. In addition, the last two peaks seemed to be shifted at 24 and 38-hour incubations. Moreover, when compared with the the samples exposed for four hours, peaks at eight-hour incubation were greater than peaks at the same time point of four hours exposure.

When 25 μT was applied for eight hours, the patterns observed were less consistent as in four hours exposure data. All caspases had peaks at eight-hour incubation, but sometimes there were other peaks at two, four and six-hour incubation periods. All peaks were smaller than the corresponding peaks from 100 μT. The decrease seen in 25 μT exposed enzymes was faster than the decrease seen in 100 μT exposed enzymes.

The common pattern observed in almost all caspases is a fast fluctuation of caspase activities between zero and eight hours. In this interval caspases generally reach their maximum values, but the fluctuations seem faster than the rest of the measured time interval.

In the second phase of the experiments, activity of each caspase was investigated when the applied magnetic field strength was kept constant, whereas exposure durations were varied (from Figure 5.10 to Figure 5.23). It can be seen from relevant figures that the patterns observed for four- and eight-hour exposures at 100 μT were very similar in each caspase. The interesting difference appears between the caspase activity curves resulting from four- and eight-hours exposure in the time interval between the 12^{th} and 38^{th} hours (after the beginning of the exposure). Within that time interval the the four- and eight-hours exposure curves fluctuate with a 180º relative phase difference, i.e. the peak of the one coincides with the bottom of the other. After

the 38th hour, the two curves start to behave in a parallel manner for each caspase decreasing gradually.

When 25 μT was applied to the HEK 293 cells for the two exposure durations, the patterns generated for each caspase were somewhat different from those produced from 100 μT data. First of all the peak heights were much lower than peak heights at 100 μT except caspase-10. Secondly, after 20-hour incubation time point, all caspase activities were found to be zero. Another important distinction is that the time shift, which can be seen in 100 μT samples, cannot be observed in 25 μT samples.

The increases in caspase activities were compared with staurosporine-induced caspases. It can be seen from Figure 5.24 and Figure 5.25 that caspase activities increase when 100 μT is applied, but this increase canot be compared with that of the staurosporine-induced samples at the same time points. When the magnetic field strength is decreased to 25 μT, caspase activities still increase except caspase-9, but again this increase is much lower than staurosporine-induced increase.

In addition to analyses made on caspase activities, trypan blue exclusion tests were performed in order to get the cell viability differences (Figure 5.26 and Figure 5.27). For the samples to which 100 μT was applied, there was no meaningful difference observed between exposed cells and sham-exposed cells. The same situation was also valid for 25 μT exposure.

6.3. Interpretation of the Results from the Perspective of the Caspase Cascade

It is widely known that caspases are activated in a cascade, and thus they play different roles in apoptosis according to a hierarchy (Figure 6.1). The cascade can be triggered either intrinsically or extrinsically. The receptor-mediated extrinsic pathway and the intrinsic pathway converge prior to the activation of the caspases.

The data presented in the framework of this thesis indicate that when 100 μT ELF-EMF is applied to the HEK 293 cells, all seven caspases investigated investigated are activated, but this activation shows an oscillatory pattern, and in the long run it

seems to be damped by some unknown intracellular mechanisms. The hierarchical activation of caspases cannot be observed from this data, because the caspase activation is achieved in the first 10 minutes of apoptosis induction [5]. Another fact which can be derived from the cell viability data is that 100 μT magnetic field strength and the two selected exposure durations are not enough to induce apoptosis in this cellular context.

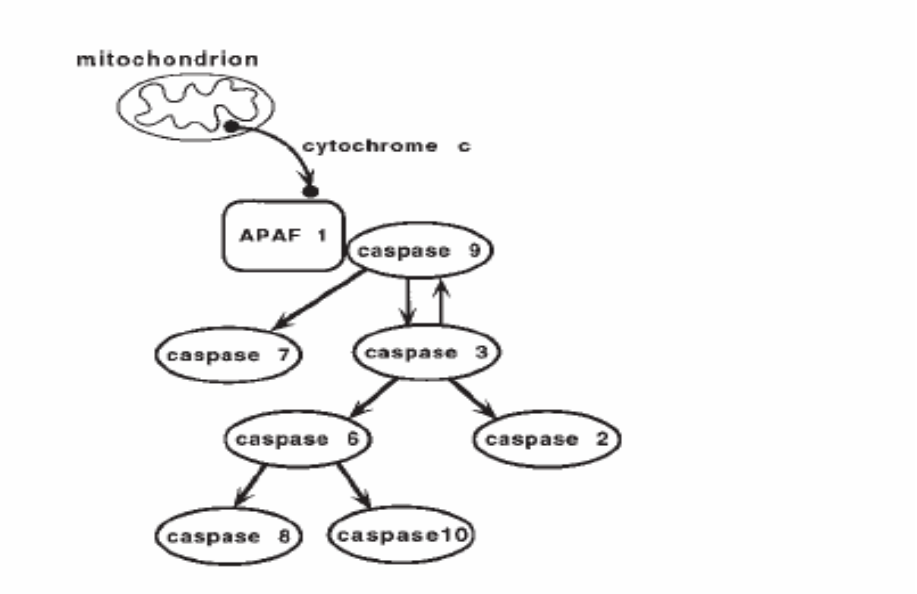

Figure 6.1. The caspase cascade [10]

Although in general it is not possible to distinguish whether the ELF-EMF triggers the caspase activities intrincisally or extrinsically because of the early convergence of both pathways, the comparison of some of the obtained results and some recent findings from the literature seem to support a receptor-mediated (extrinsic) triggering: Although Figure 6.1 shows the caspase-10 in the bottom line of the caspase activation hierarchy, meaning that caspase-10 is an executioner caspase, recent findings indicate that caspase-10 can be an apical caspase, like caspase-8, playing its role in receptor mediated apoptosis (extrinsic pathway). This pattern cannot be seen in the data resulting from 100 μT exposure. This can be a result of the high magnetic field strength, and it is not possible to observe the sequence of activation of the different caspases. However, for 25 μT exposure (Figure 5.23) only caspase-10 shows a meaningful difference from negative controls. A possible explanation of this is that 25 μT can only activate the death receptors and their closest

neighbours, like caspase-10, but the effects seem to fade out before propagating further down the pathway.

The receptor-mediated pathway hypothesis can also be supported by the fact that electrical fields generated by extremely low frequency electromagnetic fields cannot penetrate into the cells through plasma membrane, and thus only the magnetic field component of the ELF-EMFs can pass through cell membrane. On the other hand, the electric currents they induced inside the cells are too weak to trigger a measurable change. In light of this information and the data presented in this thesis, it is possible that ELF-EMFs can induce cellular changes by affecting receptors situated on the cell membrane.

7. CONCLUSIONS

According to the classification made by WHO, ELF-EMFs are categorized as "class 2B" meaning that these fields are possible carcinogens to humans. There are many epidemiological reports implying the direct effects of ELF-EMFs in carcinogenesis, especially childhood leukemia. However, epidemiological findings have their own drawbacks, because there are many variables, which are taken as constants because of the lack of extensive search, and moreover, sometimes there are some unknown factors, which play important roles in pathologies.

The animal studies conducted in laboratories have their specific problems, too. Although the experimental environment is strictly controlled in these studies, animals from the same species may respond differently in different times to ELF-EMF exposure. From this point of view, cell culture studies seem to be advantegeous, because the environment is strictly controlled, and single cells can be more easily manipulated and treated than laboratory animals. On the other hand, cell culture experiments have also some limitations, especially in extrapolating the results derived from these experiments to multicellular life. Cell lines used in the experiments are not the cells, which can be found in multicellular organisms, and because of the modifications made artificially, their behaviors may not be the same as "normal" cells. Primary cell culture studies may be problematic eventhough they are isolated directly from animal tissues. It must be kept in mind that multicellular organisms are hierarchically ordered, complex systems, and there are a vast number of regulatory mechanisms, which affect the behavior of the single cell located in a certain tissue. These regulatory mechanisms occurring at the tissue level or the level of the whole organism may affect the response of the individual cells to ELF-EMFs. Because of the absence of these mechanisms in cell cultures, these cells may respond to the same stimuli differently.

Although in vitro and in vivo studies are very essential for finding out the exact role of ELF-EMFs on biological systems, the modeling relation, which was mentioned in the beginning of this thesis, must be kept in mind. The formal systems are

constructed by experimenters in order to analyze a situation seen in the real world. During construction of the formal system, only a limited set of parameters can be taken, and inevitably the rest should be considered as constant. Moreover, there may exist some other unknown variables, which may be very important in the relevant study. Because of this limited nature of a formal system as compared to its natural counterpart, the data generated from a formal system needs to be interpreted cautiously.

APPENDIX A: DATA TABLES

Each absorbance value represents the average of nine independent measurements.

Table A.1. Average absorbance values and standard deviations of caspase-1 activity at 100, 25 μT magnetic field strengths and sham exposed cells for four hours exposure

Time (hr)	Absorbance at 100 μT		Absorbance at 25 μT		Absorbance at negative Controls	
	Average	Standard Deviation	Average	Standard Deviation	Average	Standard Deviation
0	0.097	0.003	0.097	0.003	0.097	0.003
2	0.192	0.066	0.092	0.007	0.065	0.001
4	0.243	0.0112	0.114	0.006	0.043	0.004
6	0.100	0.010	0.096	0.005	0.038	0.001
7	0.057	0.002	0.104	0.032	0.020	0.003
8	0.113	0.015	0.123	0.042	0.012	0.002
9	0.098	0.002	0.059	0.003	0.008	0.004
10	0.055	0.015	0.096	0.006	0.006	0.001
12	0.060	0.008	0.071	0.008	0.002	0.001
16	0.226	0.004	0.034	0.006	0	0
20	0.117	0.003	0.010	0.005	0	0
24	0.117	0.011	0.005	0.001	0	0
28	0.117	0.003	0	0	0	0
34	0.208	0.014	0	0	0	0
38	0.177	0.004	0	0	0	0
40	0.150	0.006	0.001	0.003	0	0
44	0.110	0.004	0	0	0	0
48	0.076	0.004	0	0	0	0
56	0.043	0.005	0	0	0	0

Table A.2. Average absorbance values and standard deviations of caspase-2 activity at 100, 25 μT magnetic field strengths and sham exposed cells for four hours exposure

Time (hr)	Absorbance at 100 μT		Absorbance at 25 μT		Absorbance at negative Controls	
	Average	Standard Deviation	Average	Standard Deviation	Average	Standard Deviation
0	0.097	0.003	0.097	0.003	0.097	0.003
2	0.149	0.054	0.114	0.044	0.080	0.001
4	0.236	0.032	0.126	0.021	0.028	0.004
6	0.138	0.045	0.089	0.006	0.009	0.001
7	0.076	0.003	0.048	0.002	0.005	0.003
8	0.132	0.078	0.140	0.035	0.003	0.002
9	0.046	0.002	0.013	0.003	0.007	0.004
10	0.029	0.006	0.105	0.021	0.007	0.001
12	0.046	0.005	0.083	0.008	0.006	0.001
16	0.216	0.061	0.025	0.003	0	0
20	0.149	0.035	0.008	0.002	0	0
24	0.128	0.052	0.001	0.005	0	0
28	0.107	0.021	0.001	0.003	0	0
34	0.206	0.056	0	0	0	0
38	0.151	0.041	0	0	0	0
40	0.120	0.021	0	0	0	0
44	0.092	0.008	0	0	0	0
48	0.048	0.004	0	0	0	0
56	0.033	0.004	0	0	0	0

Table A.3. Average absorbance values and standard deviations of caspase-3 activity at 100, 25 μT magnetic field strengths and sham exposed cells for four hours exposure

Time (hr)	Absorbance at 100 μT		Absorbance at 25 μT		Absorbance at negative Controls	
	Average	Standard Deviation	Average	Standard Deviation	Average	Standard Deviation
0	0.106	0.003	0.106	0.003	0.106	0.003
2	0.144	0.025	0.114	0.031	0.063	0.001
4	0.298	0.054	0.022	0.008	0.024	0.004
6	0.088	0.003	0.111	0.012	0.011	0.001
7	0.068	0.005	0.071	0.003	0.005	0.003
8	0.098	0.006	0.177	0.012	0.003	0.002
9	0.046	0.002	0.022	0.006	0.003	0.004
10	0.019	0.008	0.136	0.056	0.001	0.001
12	0.051	0.009	0.124	0.023	0.001	0.001
16	0.269	0.051	0.029	0.009	0	0
20	0.144	0.030	0.006	0.005	0	0
24	0.101	0.061	0	0	0	0
28	0.102	0.022	0	0	0	0
34	0.269	0.035	0	0	0	0
38	0.143	0.011	0	0	0	0
40	0.122	0.031	0	0	0	0
44	0.079	0.004	0	0	0	0
48	0.055	0.007	0	0	0	0
56	0.022	0.002	0	0	0	0

Table A.4. Average absorbance values and standard deviations of caspase-6 activity at 100, 25 μT magnetic field strengths and sham exposed cells for four hours exposure

Time (hr)	Absorbance at 100 μT		Absorbance at 25 μT		Absorbance at negative Controls	
	Average	Standard Deviation	Average	Standard Deviation	Average	Standard Deviation
0	0.111	0.003	0.111	0.003	0.111	0.003
2	0.184	0.044	0.107	0.025	0.060	0.001
4	0.236	0.026	0.104	0.017	0.027	0.004
6	0.082	0.006	0.095	0.003	0.002	0.001
7	0.067	0.004	0.029	0.002	0.001	0.003
8	0.065	0.005	0.109	0.025	0.001	0.002
9	0.046	0.001	0.010	0.005	0.001	0.004
10	0.025	0.008	0.094	0.006	0	0
12	0.038	0.003	0.110	0.028	0	0
16	0.215	0.023	0.012	0.002	0	0
20	0.142	0.014	0.002	0.005	0	0
24	0.074	0.004	0	0	0	0
28	0.108	0.027	0	0	0	0
34	0.192	0.036	0	0	0	0
38	0.136	0.045	0	0	0	0
40	0.123	0.013	0	0	0	0
44	0.086	0.008	0	0	0	0
48	0.055	0.004	0	0	0	0
56	0.022	0.002	0	0	0	0

Table A.5. Average absorbance values and standard deviations of caspase-8 activity at 100, 25 μT magnetic field strengths and sham exposed cells for four hours exposure

Time (hr)	Absorbance at 100 μT		Absorbance at 25 μT		Absorbance at negative Controls	
	Average	Standard Deviation	Average	Standard Deviation	Average	Standard Deviation
0	0.095	0.003	0.095	0.003	0.095	0.003
2	0.141	0.045	0.028	0.003	0.063	0.001
4	0.238	0.022	0.107	0.017	0.016	0.004
6	0.110	0.031	0.114	0.011	0.006	0.001
7	0.066	0.005	0.010	0.007	0.005	0.003
8	0.116	0.013	0.093	0.006	0.003	0.002
9	0.043	0.004	0.002	0.005	0.001	0.004
10	0.022	0.008	0.091	0.004	0.001	0.001
12	0.029	0.002	0.090	0.008	0	0
16	0.210	0.021	0	0	0	0
20	0.151	0.032	0	0	0	0
24	0.108	0.021	0	0	0	0
28	0.100	0.019	0	0	0	0
34	0.211	0.013	0	0	0	0
38	0.151	0.014	0.001	0.004	0	0
40	0.107	0.021	0	0	0	0
44	0.085	0.005	0	0	0	0
48	0.051	0.008	0	0	0	0
56	0.028	0.009	0	0	0	0

Table A.6. Average absorbance values and standard deviations of caspase-9 activity at 100, 25 μT magnetic field strengths and sham exposed cells for four hours exposure

Time (hr)	Absorbance at 100 μT		Absorbance at 25 μT		Absorbance at negative Controls	
	Average	Standard Deviation	Average	Standard Deviation	Average	Standard Deviation
0	0.072	0.003	0.072	0.003	0.072	0.003
2	0.118	0.022	0.004	0.007	0.050	0.001
4	0.223	0.027	0.054	0.007	0.01	0.004
6	0.070	0.005	0.037	0.002	0.001	0.001
7	0.063	0.008	0.004	0.005	0	0
8	0.071	0.008	0.016	0.004	0.001	0.002
9	0.041	0.005	0.004	0.007	0	0
10	0.012	0.009	0.008	0.007	0	0
12	0.024	0.006	0.001	0.005	0	0
16	0.210	0.022	0.001	0.006	0	0
20	0.127	0.023	0	0	0.001	0.008
24	0.073	0.003	0	0	0	0
28	0.098	0.008	0.001	0.005	0	0
34	0.178	0.021	0	0	0	0
38	0.134	0.036	0	0	0	0
40	0.107	0.025	0	0	0	0
44	0.073	0.007	0	0	0	0
48	0.040	0.006	0	0	0	0
56	0.010	0.002	0	0	0	0

Table A.7. Average absorbance values and standard deviations of caspase-10 activity at 100, 25 μT magnetic field strengths and sham exposed cells for four hours exposure

Time (hr)	Absorbance at 100 μT		Absorbance at 25 μT		Absorbance at negative controls	
	Average	Standard Deviation	Average	Standard Deviation	Average	Standard Deviation
0	0.066	0.003	0.066	0.003	0.066	0.003
2	0.108	0.025	0.100	0.027	0.057	0.001
4	0.194	0.035	0.144	0.021	0.012	0.004
6	0.059	0.005	0.148	0.056	0.001	0.001
7	0.050	0.004	0.127	0.022	0	0
8	0.040	0.009	0.206	0.032	0.001	0.002
9	0.033	0.009	0.043	0.005	0.001	0.004
10	0.007	0.005	0.130	0.028	0	0
12	0.023	0.006	0.139	0.038	0	0
16	0.192	0.026	0.092	0.008	0.001	0.006
20	0.122	0.028	0.039	0.003	0.001	0.008
24	0.055	0.001	0.010	0.003	0	0
28	0.075	0.008	0.002	0.006	0	0
34	0.177	0.025	0.001	0.008	0	0
38	0.126	0.029	0	0	0	0
40	0.105	0.013	0	0	0	0
44	0.062	0.008	0	0	0	0
48	0.034	0.007	0	0	0	0
56	0.016	0.002	0	0	0	0

Table A.8. Average absorbance values and standard deviations of caspase-1 activity at 100 μT and 25 μT magnetic field strengths and sham exposed cells for eight hours exposure

Time (hr)	Absorbance at 100 μT		Absorbance at 25 μT		Absorbance at negative Controls	
	Average	Standard Deviation	Average	Standard Deviation	Average	Standard Deviation
0	0.097	0.003	0.097	0.003	0.097	0.003
2	0.192	0.025	0.092	0.004	0.065	0.001
4	0.243	0.036	0.114	0.019	0.043	0.004
6	0.201	0.014	0.104	0.024	0.038	0.001
7	0.057	0.007	0.104	0.019	0.020	0.003
8	0.248	0.028	0.128	0.027	0.012	0.002
9	0.172	0.034	0.107	0.035	0.008	0.004
10	0.102	0.027	0.059	0.006	0.006	0.001
12	0.070	0.004	0.024	0.008	0.002	0.001
16	0.043	0.003	0.011	0.007	0	0
20	0.203	0.028	0.005	0.009	0	0
24	0.224	0.031	0.001	0.007	0	0
28	0.058	0.006	0.001	0.009	0	0
34	0.058	0.008	0	0	0	0
38	0.134	0.028	0	0	0	0
40	0.102	0.056	0	0	0	0
44	0.073	0.006	0	0	0	0
48	0.046	0.003	0	0	0	0
56	0.022	0.001	0	0	0	0

Table A.9. Average absorbance values and standard deviations of caspase-2 activity at 100 μT and 25 μT magnetic field strengths and sham exposed cells for eight hours exposure

Time (hr)	Absorbance at 100 μT		Absorbance at 25 μT		Absorbance at negative Controls	
	Average	Standard Deviation	Average	Standard Deviation	Average	Standard Deviation
0	0.097	0.003	0.097	0.003	0.097	0.003
2	0.149	0.034	0.114	0.032	0.080	0.001
4	0.236	0.014	0.126	0.021	0.028	0.004
6	0.199	0.034	0.115	0.015	0.009	0.001
7	0.076	0.009	0.048	0.003	0.005	0.003
8	0.178	0.027	0.140	0.021	0.003	0.002
9	0.146	0.029	0.133	0.035	0.001	0.004
10	0.081	0.008	0.096	0.009	0.001	0.001
12	0.048	0.009	0.035	0.006	0.001	0.001
16	0.026	0.008	0.016	0.005	0	0
20	0.032	0.001	0.007	0.009	0	0
24	0.172	0.014	0.001	0.008	0	0
28	0.150	0.025	0	0	0	0
34	0.034	0.007	0	0	0	0
38	0.101	0.030	0	0	0	0
40	0.079	0.006	0	0	0	0
44	0.055	0.005	0	0	0	0
48	0.033	0.001	0	0	0	0
56	0.014	0.003	0	0	0	0

Table A.10. Average absorbance values and standard deviations of caspase-3 activity at 100 μT and 25 μTmagnetic field strengths and sham exposed cells for eight hours exposure

Time (hr)	Absorbance at 100 μT		Absorbance at 25 μT		Absorbance at negative Controls	
	Average	Standard Deviation	Average	Standard Deviation	Average	Standard Deviation
0	0.106	0.003	0.106	0.003	0.106	0.003
2	0.144	0.028	0.114	0.019	0.063	0.001
4	0.298	0.037	0.022	0.007	0.024	0.004
6	0.172	0.023	0.119	0.028	0.011	0.001
7	0.068	0.002	0.071	0.009	0.005	0.003
8	0.162	0.028	0.153	0.031	0.003	0.002
9	0.136	0.027	0.122	0.016	0.003	0.004
10	0.080	0.005	0.073	0.007	0.001	0.001
12	0.051	0.006	0.031	0.008	0.001	0.001
16	0.015	0.001	0.013	0.005	0.001	0.008
20	0.017	0.008	0.003	0.002	0	0
24	0.150	0.028	0.002	0.008	0	0
28	0.131	0.030	0	0	0	0
34	0.028	0.008	0	0	0	0
38	0.081	0.003	0	0	0	0
40	0.060	0.001	0	0	0	0
44	0.042	0.004	0	0	0	0
48	0.025	0.008	0	0	0	0
56	0.012	0.006	0	0	0	0

Table A.11. Average absorbance values and standard deviations of caspase-6 activity at 100 μT and 25 μT magnetic field strengths and sham exposed cells for eight hours exposure

Time (hr)	Absorbance at 100 μT		Absorbance at 25 μT		Absorbance at negative Controls	
	Average	Standard Deviation	Average	Standard Deviation	Average	Standard Deviation
0	0.111	0.003	0.111	0.003	0.111	0.003
2	0.184	0.028	0.107	0.062	0.060	0.001
4	0.236	0.034	0.104	0.021	0.027	0.004
6	0.174	0.028	0.031	0.004	0.002	0.001
7	0.067	0.008	0.029	0.004	0.001	0.003
8	0.218	0.027	0.063	0.008	0.001	0.002
9	0.128	0.041	0.040	0.008	0.001	0.004
10	0.087	0.005	0.017	0.006	0	0
12	0.067	0.005	0.008	0.009	0	0
16	0.025	0.008	0.002	0.006	0	0
20	0.034	0.008	0.001	0.004	0	0
24	0.198	0.012	0	0	0	0
28	0.180	0.017	0.001	0.005	0	0
34	0.031	0.005	0	0	0	0
38	0.084	0.006	0	0	0	0
40	0.060	0.007	0	0	0	0
44	0.034	0.008	0	0	0	0
48	0.014	0.007	0	0	0	0
56	0.008	0.001	0	0	0	0

Table A.12. Average absorbance values and standard deviations of caspase-8 activity at 100 μT and 25 μT magnetic field strengths and sham exposed cells for eight hours exposure

Time (hr)	Absorbance at 100 μT		Absorbance at 25 μT		Absorbance at negative Controls	
	Average	Standard Deviation	Average	Standard Deviation	Average	Standard Deviation
0	0.095		0.095		0.095	0.003
2	0.141		0.028		0.063	0.001
4	0.238		0.107		0.016	0.004
6	0.156		0.013		0.006	0.001
7	0.066		0.010		0.005	0.003
8	0.162		0.033		0.003	0.002
9	0.124		0.020		0.001	0.004
10	0.091		0.006		0.001	0.001
12	0.050		0.002		0.001	0.001
16	0.005		0.003		0.001	0
20	0.019		0.001		0	0
24	0.162		0		0	0
28	0.141		0		0	0
34	0.014		0		0	0
38	0.063		0		0	0
40	0.045		0		0	0
44	0.028		0		0	0
48	0.014		0		0	0
56	0.006		0		0	0

Table A.13. Average absorbance values and standard deviations of caspase-9 activity at 100 μT and 25 μT magnetic field strengths and sham exposed cells for eight hours exposure

Time (hr)	Absorbance at 100 μT		Absorbance at 25 μT		Absorbance at negative Controls	
	Average	Standard Deviation	Average	Standard Deviation	Average	Standard Deviation
0	0.072		0.072		0.072	0.003
2	0.118		0.004		0.050	0.001
4	0.223		0.054		0.010	0.004
6	0.163		0.007		0.001	0.001
7	0.063		0.004		0	0.003
8	0.145		0.011		0.001	0.002
9	0.105		0.007		0	0.004
10	0.059		0.002		0	0.001
12	0.028		0		0	0.001
16	0.005		0		0.001	0
20	0.013		0		0.001	0
24	0.125		0		0	0
28	0.105		0		0	0
34	0.007		0		0	0
38	0.051		0		0	0
40	0.033		0		0	0
44	0.020		0		0	0
48	0.010		0		0	0
56	0.003		0		0	0

Table A.14. Average absorbance values and standard deviations of caspase-10 activity at 100 μT and 25 μT magnetic field strengths and sham exposed cells for eight hours exposure

Time (hr)	Absorbance at 100 μT		Absorbance at 25 μT		Absorbance at negative Controls	
	Average	Standard Deviation	Average	Standard Deviation	Average	Standard Deviation
0	0.066		0.066		0.066	0.003
2	0.108		0.100		0.057	0.001
4	0.194		0.144		0.012	0.004
6	0.139		0.146		0.001	0.001
7	0.050		0.127		0	0.003
8	0.140		0.206		0.001	0.002
9	0.114		0.152		0.001	0.004
10	0.073		0.082		0	0.001
12	0.047		0.042		0	0.001
16	0.002		0.020		0.001	0
20	0.013		0.006		0.001	0
24	0.138		0.002		0	0
28	0.120		0		0	0
34	0.008		0		0	0
38	0.062		0		0	0
40	0.043		0		0	0
44	0.027		0		0	0
48	0.013		0		0	0
56	0.005		0		0	0

Table A.15. Average absorbance values and standard deviations of caspase-1 activity at 100 μT magnetic field strength and sham exposed cells for four and eight hours exposure

Time (hr)	Four Hour Exposure	Eight Hour Exposure	Negative Controls
0	0.097	0.097	0.097
2	0.192	0.192	0.065
4	0.243	0.243	0.043
6	0.100	0.201	0.038
7	0.057	0.057	0.020
8	0.113	0.248	0.012
9	0.098	0.172	0.008
10	0.055	0.102	0.006
12	0.060	0.070	0.002
16	0.226	0.043	0
20	0.117	0.203	0
24	0.117	0.224	0
28	0.117	0.058	0
34	0.208	0.058	0
38	0.177	0.134	0
40	0.150	0.102	0
44	0.110	0.073	0
48	0.076	0.046	0
56	0.043	0.022	0

Table A.16. Average absorbance values and standard deviations of caspase-2 activity at 100 μT magnetic field strength and sham exposed cells for four and eight hours exposure

Time (hr)	Four Hour Exposure	Eight Hour Exposure	Negative Controls
0	0.097	0.097	0.097
2	0.149	0.149	0.080
4	0.236	0.236	0.028
6	0.138	0.199	0.009
7	0.076	0.076	0.005
8	0.132	0.178	0.003
9	0.046	0.146	0.001
10	0.029	0.081	0.001
12	0.046	0.048	0.001
16	0.216	0.026	0
20	0.149	0.032	0
24	0.128	0.172	0
28	0.107	0.150	0
34	0.206	0.034	0
38	0.151	0.101	0
40	0.120	0.079	0
44	0.092	0.055	0
48	0.048	0.033	0
56	0.033	0.014	0

Table A.17. Average absorbance values and standard deviations of caspase-3 activity at 100 μT magnetic field strength and sham exposed cells for four and eight hours exposure

Time (hr)	Four Hour Exposure	Eight Hour Exposure	Negative Controls
0	0.106	0.106	0.106
2	0.144	0.144	0.060
4	0.298	0.298	0.024
6	0.088	0.172	0.011
7	0.068	0.068	0.005
8	0.098	0.162	0
9	0.046	0.136	0
10	0.019	0.080	0.001
12	0.051	0.051	0.001
16	0.269	0.015	0.001
20	0.144	0.017	0
24	0.101	0.150	0
28	0.102	0.131	0
34	0.269	0.028	0
38	0.143	0.081	0
40	0.122	0.060	0
44	0.079	0.042	0
48	0.055	0.025	0
56	0.022	0.012	0

Table A.18. Average absorbance values and standard deviations of caspase-6 activity at 100 μT magnetic field strength and sham exposed cells for four and eight hours exposure

Time (hr)	Four Hour Exposure	Eight Hour Exposure	Negative Controls
0	0.111	0.111	0.111
2	0.184	0.184	0.060
4	0.236	0.236	0.027
6	0.082	0.174	0.002
7	0.067	0.067	0.001
8	0.065	0.218	0.001
9	0.046	0.128	0.001
10	0.025	0.087	0
12	0.038	0.067	0
16	0.215	0.025	0
20	0.142	0.034	0
24	0.074	0.198	0
28	0.108	0.180	0
34	0.192	0.031	0
38	0.136	0.084	0
40	0.123	0.060	0
44	0.086	0.034	0
48	0.055	0.014	0
56	0.022	0.008	0

Table A.19. Average absorbance values and standard deviations of caspase-8 activity at 100 μT magnetic field strength and sham exposed cells for four and eight hours exposure

Time (hr)	Four Hour Exposure	Eight Hour Exposure	Negative Controls
0	0.095	0.095	0.095
2	0.141	0.141	0.063
4	0.238	0.238	0.016
6	0.110	0.156	0.006
7	0.066	0.066	0.005
8	0.116	0.162	0.003
9	0.043	0.124	05
10	0.022	0.091	0.001
12	0.029	0.050	0
16	0.210	0.005	0
20	0.151	0.019	0
24	0.108	0.162	0
28	0.100	0.141	0
34	0.211	0.014	0
38	0.151	0.063	0
40	0.107	0.045	0
44	0.085	0.028	0
48	0.051	0.014	0
56	0.028	0.006	0

Table A.20. Average absorbance values and standard deviations of caspase-9 activity at 100 μT magnetic field strength and sham exposed cells for four and eight hours exposure

Time (hr)	Four Hour Exposure	Eight Hour Exposure	Negative Controls
0	0.072	0.072	0.072
2	0.118	0.118	0.050
4	0.223	0.223	0.010
6	0.070	0.163	0.001
7	0.063	0.063	0
8	0.071	0.145	0.001
9	0.041	0.105	0
10	0.012	0.059	0
12	0.024	0.028	0
16	0.210	0.005	0.001
20	0.127	0.013	0.001
24	0.073	0.125	0
28	0.098	0.105	0
34	0.178	0.007	0
38	0.134	0.051	0
40	0.107	0.033	0
44	0.073	0.020	0
48	0.040	0.010	0
56	0.010	0.002	0

Table A.21. Average absorbance values and standard deviations of caspase-10 activity at 100 μT magnetic field strength and sham exposed cells for four and eight hours exposure

Time (hr)	Four Hour Exposure	Eight Hour Exposure	Negative Controls
0	0.066	0.066	0.066
2	0.108	0.108	0.057
4	0.194	0.194	0.012
6	0.059	0.139	0.001
7	0.050	0.050	0
8	0.040	0.140	0.001
9	0.033	0.114	0.001
10	0.007	0.073	0
12	0.023	0.047	0
16	0.192	0.002	0.001
20	0.122	0.013	0.001
24	0.055	0.138	0
28	0.075	0.120	0
34	0.177	0.008	0
38	0.126	0.062	0
40	0.105	0.043	0
44	0.062	0.027	0
48	0.034	0.013	0
56	0.016	0.004	0

Table A.22. Average absorbance values and standard deviations of caspase-1 activity at 25 μT magnetic field strength and sham exposed cells for four and eight hours exposure

Time (hr)	Four Hour Exposure	Eight Hour Exposure	Negative Controls
0	0.097	0.097	0.097
2	0.092	0.092	0.065
4	0.114	0.114	0.043
6	0.096	0.104	0.038
7	0.104	0.104	0.020
8	0.123	0.128	0.012
9	0.059	0.107	0.008
10	0.096	0.059	0.006
12	0.071	0.024	0.002
16	0.034	0.011	0
20	0.010	0.005	0
24	0.005	0.001	0
28	0	0.001	0
34	0	0	0
38	0	0	0
40	0	0	0
44	0	0	0
48	0	0	0
56	0	0	0

Table A.23. Average absorbance values and standard deviations of caspase-2 activity at 25 μT magnetic field strength and sham exposed cells for four and eight hours exposure

Time (hr)	Four Hour Exposure	Eight Hour Exposure	Negative Controls
0	0.097	0.097	0.097
2	0.114	0.114	0.080
4	0.126	0.126	0.028
6	0.089	0.115	0.009
7	0.048	0.048	0.005
8	0.140	0.140	0.003
9	0.013	0.133	0.001
10	0.105	0.096	0.001
12	0.083	0.035	0.001
16	0.025	0.016	0
20	0.008	0.007	0
24	0.001	0.001	0
28	0.001	0	0
34	0	0	0
38	0	0	0
40	0	0	0
44	0	0	0
48	0	0	0
56	0	0	0

Table A.24. Average absorbance values and standard deviations of caspase-3 activity at 25 μT magnetic field strength and sham exposed cells for four and eight hours exposure

Time (hr)	Four Hour Exposure	Eight Hour Exposure	Negative Controls
0	0.106	0.106	0.106
2	0.114	0.114	0.063
4	0.022	0.022	0.024
6	0.111	0.119	0.011
7	0.071	0.071	0.005
8	0.177	0.153	0.003
9	0.022	0.122	0.003
10	0.136	0.073	0.001
12	0.124	0.031	0.001
16	0.029	0.013	0.001
20	0.006	0.003	0
24	0	0.002	0
28	0	0	0
34	0	0	0
38	0	0	0
40	0	0	0
44	0	0	0
48	0	0	0
56	0	0	0

Table A.25. Average absorbance values and standard deviations of caspase-6 activity at 25 μT magnetic field strength and sham exposed cells for four and eight hours exposure

Time (hr)	Four Hour Exposure	Eight Hour Exposure	Negative Controls
0	0.111	0.111	0.111
2	0.107	0.107	0.060
4	0.104	0.104	0.027
6	0.095	0.031	0.002
7	0.029	0.029	0.001
8	0.109	0.063	0.001
9	0.010	0.040	0.001
10	0.094	0.017	0
12	0.110	0.008	0
16	0.012	0.002	0
20	0.002	0.001	0
24	0	0	0
28	0.001	0.001	0
34	0	0	0
38	0	0	0
40	0	0	0
44	0	0	0
48	0	0	0
56	0	0	0

Table A.26. Average absorbance values and standard deviations of caspase-8 activity at 25 μT magnetic field strength and sham exposed cells for four and eight hours exposure

Time (hr)	Four Hour Exposure	Eight Hour Exposure	Negative Controls
0	0.095	0.095	0.095
2	0.028	0.028	0.063
4	0.107	0.107	0.016
6	0.114	0.013	0.006
7	0.010	0.010	0.005
8	0.093	0.033	0.003
9	0.002	0.020	0.001
10	0.091	0.006	0.001
12	0.090	0.001	0
16	0.004	0.002	0
20	0.001	0.001	0
24	0	0	0
28	0	0	0
34	0	0	0
38	0.001	0	0
40	0	0	0
44	0	0	0
48	0	0	0
56	0	0	0

Table A.27. Average absorbance values and standard deviations of caspase-9 activity at 25 μT magnetic field strength and sham exposed cells for four and eight hours exposure

Time (hr)	Four Hour Exposure	Eight Hour Exposure	Negative Controls
0	0.072	0.072	0.072
2	0.004	0.004	0.050
4	0.054	0.054	0.010
6	0.037	0.007	0.001
7	0.004	0.004	0
8	0.016	0.011	0.001
9	0.004	0.007	0
10	0.008	0.002	0
12	0.001	0	0
16	0.001	0	0.001
20	0	0	0.001
24	0	0	0
28	0.001	0	0
34	0	0	0
38	0	0	0
40	0	0	0
44	0	0	0
48	0	0	0
56	0	0	0

Table A.28. Average absorbance values and standard deviations of caspase-10 activity at 25 μT magnetic field strength and sham exposed cells for four and eight hours exposure

Time (hr)	Four Hour Exposure	Eight Hour Exposure	Negative Controls
0	0.066	0.066	0.066
2	0.100	0.100	0.057
4	0.144	0.144	0.012
6	0.148	0.146	0.001
7	0.127	0.127	0
8	0.206	0.206	0.001
9	0.043	0.152	0.001
10	0.130	0.082	0
12	0.139	0.042	0
16	0.092	0.020	0.001
20	0.039	0.006	0.001
24	0.010	0.002	0
28	0.002	0	0
34	0.001	0	0
38	0	0	0
40	0	0	0
44	0	0	0
48	0	0	0
56	0	0	0

Table A.29. Caspase activities from sham exposed cells at four hour incubation time

Caspase Name	Average Absorbance (405nm)	Standard Deviation
Caspase-1	0.043	0.003
Caspase-2	0.028	0.001
Caspase-3	0.024	0.001
Caspase-6	0.027	0.002
Caspase-8	0.016	0.001
Caspase-9	0.010	0.001
Caspase-10	0.012	0.002

Table A.30. Caspase activities from 100 μT exposed cells at four hour incubation time

Caspase Name	Average Absorbance (405nm)	Standard Deviation
Caspase-1	0.243	0.011
Caspase-2	0.236	0.016
Caspase-3	0.298	0.027
Caspase-6	0.236	0.007
Caspase-8	0.238	0.033
Caspase-9	0.223	0.029
Caspase-10	0.194	0.014

Table A.31. Caspase activities from 25 μT exposed cells at four hour incubation time

Caspase Name	Average Absorbance (405nm)	Standard Deviation
Caspase-1	0.114	0.004
Caspase-2	0.126	0.002
Caspase-3	0.132	0.025
Caspase-6	0.128	0.020
Caspase-8	0.065	0.011
Caspase-9	0.011	0.010
Caspase-10	0.144	0.005

Table A.32. Caspase activities from staurosporine-induced cells at four hour incubation time

Caspase Name	Average Absorbance (405nm)	Standard Deviation
Caspase-1	0.937	0.032
Caspase-2	0.997	0.011
Caspase-3	1.052	0.004
Caspase-6	1.019	0.011
Caspase-8	1.008	0.007
Caspase-9	1.003	0.011
Caspase-10	1.025	0.003

Table A.33. Cell viability data for 100 μT; four hours exposure; staurosporine-induced; sham exposed cells

Time (hr)	Per cent viability of 100 μT exposed cells	Per cent viability of staurosporine-induced cells	Per cent viability of sham exposed cells
4	0.881	0.091	0.894
6	0.874	0.091	0.872
7	0.869	0.091	0.890
8	0.846	0.091	0.854
10	0.852	0.091	0.848
12	0.875	0.091	0.876
16	0.896	0.091	0.894
20	0.902	0.091	0.8984
24	0.919	0.091	0.917
28	0.885	0.091	0.880
34	0.897	0.091	0.902
38	0.901	0.091	0.902
40	0.889	0.091	0.892
44	0.908	0.091	0.910
48	0.896	0.091	0.901
56	0.893	0.091	0.895

Table A.34. Cell viability data for 100 μT; eight hours exposure; staurosporine-induced; sham exposed cells

Time (hr)	Per cent viability of 100 μT exposed cells	Per cent viability of staurosporine-induced cells	Per cent viability of sham exposed cells
8	0.850	0.091	0.847
9	0.843	0.091	0.839
10	0.910	0.091	0.915
12	0.803	0.091	0.812
16	0.882	0.091	0.881
20	0.912	0.091	0.914
24	0.884	0.091	0.887
28	0.887	0.091	0.887
34	0.904	0.091	0.904
38	0.892	0.091	0.895
40	0.897	0.091	0.901
44	0.895	0.091	0.899
48	0.899	0.091	0.900
56	0.915	0.091	0.909

Table A.35. Cell viability data for 25 μT; four hours exposure; staurosporine-induced; sham exposed cells

Time (hr)	Per cent viability of 25 μT exposed cells	Per cent viability of staurosporine-induced cells	Per cent viability of sham exposed cells
4	0.8551	0.091	0.894
6	0.874	0.091	0.872
7	0.851	0.091	0.890
8	0.872	0.091	0.854
10	0.829	0.091	0.848
12	0.872	0.091	0.876
16	0.896	0.091	0.894
20	0.864	0.091	0.898
24	0.919	0.091	0.917
28	0.882	0.091	0.880
34	0.897	0.091	0.902
38	0.893	0.091	0.902
40	0.889	0.091	0.892
44	0.902	0.091	0.910
48	0.896	0.091	0.901
56	0.905	0.091	0.895

Table A.36. Cell viability data for 25 μT; eight hours exposure; staurosporine-induced; sham exposed cells

Time (hr)	Per cent viability of 25 μT exposed cells	Per cent viability of staurosporine-induced cells	Per cent viability of sham exposed cells
8	0.852	0.091	0.847
9	0.871	0.091	0.839
10	0.874	0.091	0.915
12	0.879	0.091	0.812
16	0.890	0.091	0.881
20	0.907	0.091	0.914
24	0.874	0.091	0.887
28	0.896	0.091	0.887
34	0.906	0.091	0.904
38	0.908	0.091	0.895
40	0.889	0.091	0.901
44	0.906	0.091	0.899
48	0.900	0.091	0.900
56	0.903	0.091	0.909

REFERENCES

1. Mikulecky, D. C., *The Modeling Relation: How We Perceive*, http://www.people.vcu.edu/~mikuleck/modrelisss.html, 2005.

2. Ameisen, J. C., "On the Origin, Evolution, and Nature of Programmed Cell Death: A Timeline of Four Billion Years", *Cell Death and Differentiation*, Vol. 9, pp. 367-393, 2002.

3. Koonin, E. V. and L. Aravind, "Origin and Evolution of Eukaryotic Apoptosis: The Bacterial Connection", *Cell Death and Differentiation*, Vol. 9, pp. 394-404, 2002.

4. Philchenkov, A., "Caspases: Potential Targets for Regulating Cell Death", *J. Cell. Mol. Med.*, Vol. 8, No. 4, pp. 432-444, 2004.

5. Green, D. R., "Apoptotic Pathways: Ten Minutes to Death", *Cell*, Vol. 121, pp. 671-674, June 2005.

6. Green, D. R., "Apoptotic Pathways: Paper Wraps Stone Blunts Scissors", *Cell*, Vol. 102, pp. 1-4, July 2000.

7. Danial, N. N. And S. J. Korsmeyer, "Cell Death: Critical Control Points", *Cell*, Vol. 116, pp. 205-219, January 2004.

8. Jacobson, M. D., M. Weil and M. C. Raff, "Programmed Cell Death in Animal Development", *Cell*, Vol. 88, pp.347-354, February 1997.

9. Riedl, S. J. And Y. Shi, "Molecular Mechanisms of Caspase Regulation During Apoptosis", *Nat. Rev. Mol. Cell Biol.*, Vol. 5, pp. 897-907, November 2004.

10. Slee, E. A., M. T. Harte, R. M. Kluck, B. B. Wolf, C. A. Casiano, D. D. Newmeyer, H. G. Wang, J. C. Reed, D. W. Nicholson, E. S. Alnemri, D. R. Green and S. J. Martin, "Ordering the Cytochrome c-Initiated Caspase Cascade: Hierarchical Activation of Caspases-2, -3, -6, -7, -8, and -10 in a Caspase-9-Dependent Manner", *The Journal of Cell Biology*, Vol. 144, No. 2, pp. 281-292, January 1999.

11. Johnson, C. R. And W. D. Jarvis, "Caspase-9 Regulation: An Update", *Apoptosis*, Vol. 9, No. 4, pp. 423-427, 2004.

12. Slee, E. A., C. Adrain and S. J. Martin, "Executioner Caspase-3, -6, and -7 Perform Distinct, Non-Redundant Roles During the Demolition Phase of Apoptosis", *The Journal of Biological Chemistry*, Vol. 276, No. 10, pp. 7320-7326, March 2001.

13. Kroemer, G., B. Dallaporta and M. Resche-Rigon, "The Mitochondrial Death/Life Regulator in Apoptosis and Necrosis", *Annual Review of Physiology*, Vol. 60, pp. 619-642, 1998.

14. Antonsson, B., S. Montessuit, B. Sanchez and J. C. Martinou, "Bax is Present as a High Molecular Weight Oligomer/Complex in the Mitochondrial Membrane of Apoptotic Cells", *The Journal of Biological Chemistry*, Vol. 276, No. 15, pp. 11615-11623, April 2001.

15. Antonsson, B., S. Montessuit, S. Lauper, R. Eskes and J. C. Martinou," Bax Oligomerization is Required for Channel-Forming Activity in Liposomes and to Trigger Cytochrome c Release from Mitochondria", *Biochem. J.*, Vol. 345, pp. 271-278, 2000.

16. Li, P., D. Nijhawan, I. Budihardjo, S. M. Srinivasula, M. Ahmad, E. S. Alnemri and X. Wang, "Cytochrome c and dATP-Dependent Formation of Apaf-1/Caspase-9 Complex Initiates an Apoptotic Protease Cascade", *Cell*, Vol. 91, pp. 479-489, November 1997.

17. Bossy-Wetzel, E. And D. R. Green, "Caspases Induce Cytochrome c Release from Mitochondria by Activating Cytosolic Factors", *The Journal of Biological Chemistry*, Vol. 274, No. 25, pp. 17484-17490, June 1999.

18. Cain, K., S. B. Bratton, C. Langlais, G. Walker, D. G. Brown, X. M. Sun and G. M. Cohen, "Apaf-1 Oligomerizes into Biologically Active ~700-kDa and Inactive ~1.4-Mda Apoptosome Complexes", *The Journal of Biological Chemistry*, Vol. 275, No. 9, pp. 6067-6070, March 2000.

19. Zamzami, N. and G. Kroemer, "The Mitochondrion in Apoptosis: How Pandora's Box Opens", *Nat. Rev. Mol. Cell Biol.*, Vol. 2, pp. 67-71, January 2001.

20. Verschaeve, L. And A. Maes, "Genetic, Carcinogenic and Teratogenic Effects of Radiofrequency Fields", *Mutation Research*, Vol. 410, pp. 141-165, 1998.

21. Adey, W. R., *Electromagnetic Fields, the Modulation of Brain Tissue Functions-A Possible Paradigm Shift in Biology*, http://www.emrnetwork.org/research/adey_encneuro_emfs.pdf, 2003.

22. Repacholi, M. H., "WHO's Health Risk Assessment of ELF Fields", *Radiation Protection Dosimetry*, Vol. 106, No. 4, pp. 297-299, 2003.

23. Huuskonen, H., M. L. Lindbohm and J. Juutilainen, "Teratogenic and Reproductive Effects of Low-Frequency Magnetic Fields", *Mutation Research*, Vol. 410, pp. 167-183, 1998.

24. Löscher, W. And R. P. Liburdy, "Animal and Cellular Studies on Carcinogenic Effects of Low Frequency (50/60-Hz) Magnetic Fields", *Mutation Research*, Vol. 410, pp. 185-220, 1998.

25. Luben, R. A., "Effects of Low-Energy Electromagnetic Fields (pulsed and DC) on Membrane Signal Transduction Processes in Biological Systems", *Health Phys.*, Vol. 61, pp. 15-28, 1991.

26. Luben, R. A., "Effects of Low-Energy Electromagnetic Fields (EMF) on Signal transduction by G Protein Linked Receptors", in M. Blank (ed.), *Electricity and Magnetism in Biology and Medicine*, pp. 57-62, San Francisco Press, San Francisco, 1993.

27. Luben, R. A., "Membrane Signal transduction as a Site of Electromagnetic Field Actions in Bone and Other Tissues", in A. H. Frey (ed.), *On the Nature of Electromagnetic Field interactions with Biological Systems*, pp. 83-98, Austin, TX, 1994.

28. Monti, M. G., L. Pernecco, M. S. Moruzzi, R. Battini, P. Zaniol and B. Barbiroli, "Effect of ELF Pulsed Electromagnetic Fields on Protein Kinase C Activation Process in HL-60 Leukemia Cells", *J. Bioelectricity*, Vol. 10, pp. 119-130, 1991.

29. Monti, M. G., L. Pernecco, M. S. Moruzzi, R. Battini, P. Zaniol and B. Barbiroli, "Extremely Low Frequency Electromagnetic Fields Stimulate Activation of Protein Kinase C in HL-60 Leukemia Cells by Increasing Membrane Transport of Calcium", in M. Blank (ed.), *Electricity and Magnetism in Biology and Medicine*, pp. 522-524, San Francisco Press, San Francisco, 1993.

30. Garcia-Sancho, J., M. Montero, J. Alvarez, R. J. Fonteriz and A. Sanchez, "Effects of Extremely Low Frequency Electromagnetic Fields on Ion Transport in Several Mammalian Cells", *Bioelectromagnetics*, Vol. 15, pp. 579-588, 1994.

31. Goodman, R. And A. S. Henderson, "Exposure of Human Cells to Electromagnetic Fields: Effect of Time and Field Strength on Transcript Levels", *Electro-Magnetobiol.*, Vol. 11, pp. 11-28, 1992.

32. Litovitz, T. A., D. Krause and J. M. Mullins, "Effect of Coherence Time of the Applied Magnetic Field on Ornithine Decarboxylase Activity", *Biochem. Biophys. Res. Commun.*, Vol. 178, pp. 862-865, 1991.

33. Mattsson, M. O., U. Rehnhom and K. H. Mild, "Gene Expression in Tumor Cells After Exposure to a 50 Hz Sinusoidal Magnetic Field", in M. Blank (ed.), *Electricity and Magnetism in Biology and Medicine*, pp. 500-502, San Francisco Press, San Francisco, 1993.

34. Liburdy, R. P., T. R. Sloma, R. Sokolic and P. Yaswen, "ELF Magnetic Fields, Breast Cancer and Melatonin: 60 Hz Fields Block Melatonin's Oncostatic Action on ER and Breast Cancer Cell Proliferation", *J. Pineal Res.*, Vol. 14, pp. 89-97, 1993.

35. Blank, M. and R. Goodman, "Electromagnetic Fields May Act Directly on DNA", *Journal of Cellular Biochemistry*, Vol. 75, pp. 369-374, 1999.

36. Blank, M. and R. Goodman, "Do Electromagnetic Fields Interact Directly with DNA?", *Bioelectromagnetics*, Vol. 18, pp. 111-115, 1997.

37. Sollazzo, V., G. C. Traina, M. DeMattei, A. Pellati, F. Pezzetti and A. Caruso, "Responses of Human MG-63 Osteosarcoma Cell Line and Human Osteoblast-Like Cells to Pulsed Electromagnetic Fields", *Bioelectromagnetics*, Vol. 18, pp. 541-547, 1997.

38. Campbell-Beachler, M., T. Ishida-Jones, W. Haggren and J. L. Phillips, "Effect of 60 Hz Magnetic Field Exposure on C-Fos Expression in Stimulated PC12 Cells", *Molecular and Cellular Biochemistry*, Vol. 189, pp. 107-111, 1998.

39. Ansari, R. M. And T. K. Hei, "Effects of 60 Hz Extremely Low Frequency Magnetic Fields (EMF) on Radiation- and Chemical-Induced Mutagenesis in Mammalian Cells", *Carcinogenesis*, Vol. 21, No. 6, pp. 1221-1226, 2000.

40. Harland, J. D. And R. P. Liburdy, "Environmental Magnetic Fields Inhibit the Antiproliferative Action of Tamoxifen and Melatonin in a Human Breast Cancer Cell Line", *Bioelectromagnetics*, Vol. 18, pp. 555-562, 1997.

41. Wei, M., M. Guizzetti, M. Yost and L. G. Costa, "Exposure to 60-Hz Magnetic Fields and Proliferation of Human Astrocytoma Cells in vitro", *Toxicology and Applied Pharmacology*, Vol. 162, pp. 166-176, 2000.

42. Schimmelpfeng, J. and H. Dertinger, "Action of a 50 Hz Magnetic Field on Proliferation of Cells in Culture", *Bioelectromagnetics*, Vol. 18, pp. 177-183, 1997.

43. Lai, H. And N. P. Singh, "Acute Exposure to a 60 Hz Magnetic Field Increases DNA Strand Breaks in Rat Brain Cells", *Bioelectromagnetics*, Vol. 18, pp. 156-165, 1997.

44. Simko, M., R. Kriehuber, D. G. Weiss and R. A. Luben, "Effects of 50 Hz EMF Exposure on Micronucleus Formation and Apoptosis in transformed and Nontransformed Human Cell Lines", *Bioelectromagnetics*, Vol. 19, pp. 85-91, 1998.

45. Blumenthal, N. C., J. Ricci, L. Breger, A. Zychlinsky, H. Solomon, G. G. Chen, D. Kuznetsov and R. Dorfman, "Effects of Low-Intensity AC and/or DC Electromagnetic Fields on Cell Attachment and Induction of Apoptosis", *Bioelectromagnetics*, Vol. 18, pp. 264-272, 1997.

46. Tofani, S., D. Barone, M. Cintorino, M. M. De Santi, A. Ferrara, R. Orlassino, P. Ossola, F. Peroglio, K. Rolfo and F. Ronchetto, "Static and ELF Magnetic Fields Induce Tumor Growth Inhibition and Apoptosis", *Bioelectromagnetics*, Vol. 22, pp. 419-428, 2001.

47. Pirozzoli, M. C., C. Marino, G. A. Lovisolo, C. Laconi, L. Mosiello and A. Negroni, "Effects of 50 Hz Electromagnetic Field Exposure on Apoptosis and Differentiation in a Neuroblastoma Cell Line", *Bioelectromagnetics*, Vol. 24, pp. 510-516, 2003.

48. Palumbo, R., D. Capasso, F. Brescia, P. Mita, M. Sarti, F. Bersani and M. R. Scarfi, "Effects on Apoptosis and Reactive Oxygen Species Formation by Jurkat Cells

Exposed to 50 Hz Electromagnetic Fields", *Bioelectromagnetics*, Vol. 27, pp. 159-162, 2006.